PHILOSOPHICAL TRANSACTIONS OF THE ROYAL SOCIETY A MATHEMATICAL, PHYSICAL & ENGINEERING SCIENCES

Igneous History of the Andean Cordillera and Patagonian Plateau around Latitude 46 degrees S

P. E. Baker, W. J. Rea, J. Skarmeta, R. Caminos and D. C. Rex

Phil. Trans. R. Soc. Lond. A 1981 **303**, 105-149
doi: 10.1098/rsta.1981.0194

Phil. Trans. R. Soc. Lond. A **303**, 105–149 (1981) [105]
Printed in Great Britain

IGNEOUS HISTORY OF THE ANDEAN CORDILLERA AND PATAGONIAN PLATEAU AROUND LATITUDE 46°S

By P. E. BAKER†[1], W. J. REA‡[2], J. SKARMETA§, R. CAMINOS‖ and D. C. REX¶

† *Department of Geology, University of Nottingham, University Park, Nottingham NG7 2RD, U.K.*
‡ *Department of Geology and Physical Sciences, Oxford Polytechnic, Headington, Oxford OX3 0BP, U.K.*
§ *Instituto de Investigaciones Geologicas, Augustinas 785, 6° piso, Santiago, Chile*
‖ *Servicio Geologico Nacional, Avda Santa Fe 1548, 2° piso, Buenos Aires, Argentina*
¶ *Department of Earth Sciences, University of Leeds, Leeds LS2 9JT, U.K.*

(*Communicated by Sir Vivian Fuchs, F.R.S. – Received 20 February* 1981)

[Plates 1 and 2]

CONTENTS

[1] Formerly at Department of Earth Sciences, University of Leeds, Leeds LS2 9JT, U.K.
[2] Formerly at Department of Geology, University College of Wales, Aberystwyth, Dyfed SW23 3DB, U.K.

From the Middle Jurassic onwards persistent igneous activity in the southern Andes around 46 °S was controlled by easterly dipping subduction along the Pacific margin. Cogenetic plutonic rocks belonging to the Patagonian batholith, and calc-alkaline volcanics ranging from basaltic andesites to rhyolitic tuffs and ignimbrites are the principal products. Erosion of the primary volcanics has led at various times to the development of thick volcaniclastic sequences, for example in the Cretaceous–Lower Tertiary Divisadero formation. The Coyhaique region marks the northerly extension of a narrow back-arc basin in which the marine Neocomian successions accumulated. Volcaniclastics from the island arc, which presumably lay to the west, are intercalated with the sediments. Although the marine basin was short-lived a mildly extensional back-arc régime may have existed through much of Mesozoic–Recent times. Widespread basalt–rhyolite volcanism on the eastern side of the cordillera seems to have been associated with this tectonic environment.

Remnants of the Patagonian basalt plateau at latitude 45–47 °S extend from the Argentine–Chile frontier to Lago Colhue Huapi. Four principal age and compositional groups have been distinguished in the lavas. (i) The oldest, which are about 80 Ma, occur in sections at Senguerr and Morro Negro. They are almost exclusively tholeiitic, but show some calc-alkaline affinities and resemble in other respects basalts from marginal basins. (ii) The second group (57–43 Ma) occur in the lower part of the Chile Chico section with a compositional spread from olivine tholeiites through alkali basalts to one occurrence of a basanite. (iii) The upper part of the main plateau sequence, where the flows are in the range 25–9 Ma, are dominantly of alkali basalt composition. (iv) Post-plateau flows from small cinder cones on the surface of the plateau range in age from *ca.* 4 Ma to 0.2 Ma or less. They are mostly highly undersaturated basanites, with occasional leucite basanites, enriched in incompatible elements. A few of the earlier tholeiites with calc-alkali traits may have been closely associated with subduction or marginal basin processes. The younger lavas are more alkalic intraplate types generated in the remote back-arc extensional zone.

Introduction

This report presents the results of an international geological expedition in Patagonia and the southern Andes, sponsored by the Royal Society in collaboration with the National Research Councils of Argentina (CONICET) and Chile (CONICYT). The expedition had two major objectives, the results of which constitute the two parts of this paper:

(*a*) to study the major igneous events in the Mesozoic and Cainozoic record of the Andean cordillera at about 46 °S in Aisen Province;

(*b*) to investigate the basaltic lava sequence of the Patagonian plateau at the same latitude.

Figure 1 shows the general location of the area studied and illustrates the approximate distribution of the plateau basalts.

The expedition travelled extensively in Patagonia, and rocks of the cordillera were examined at localities between about 45 °S and 47 °S.

The principal area of investigation was around Coyhaique where the regional stratigraphy has been established by Skarmeta (1974), but the sections of Jurassic volcanics around Puerto Ibañez were also studied in some detail. Elsewhere, observations were confined mainly to the cordilleran rocks that immediately underlie the plateau basalts. Although the essential geology of this part of the southern Andes consists of the Patagonian batholith flanked to both west and east by Mesozoic to Cainozoic volcano–sedimentary successions (Skarmeta 1978) the work described here deals almost entirely with the eastern succession. Only a few observations were made on the western margin of the batholith.

Cordilleran rocks and igneous events are considered in relation to stratigraphic studies made

in Aisen by one of the Chilean geologists on the expedition (Skarmeta 1974, 1978). Comparisons are also made with sequences established in other parts of the southern Andes (see, for example, Dalziel *et al.* 1974, Bruhn *et al.* 1979).

Results of the work on the plateau basalts constitute the second part of this paper, though a brief review (Baker & Rea 1978) and isotopic and rare earth element data (Hawkesworth *et al.* 1979) have already been published.

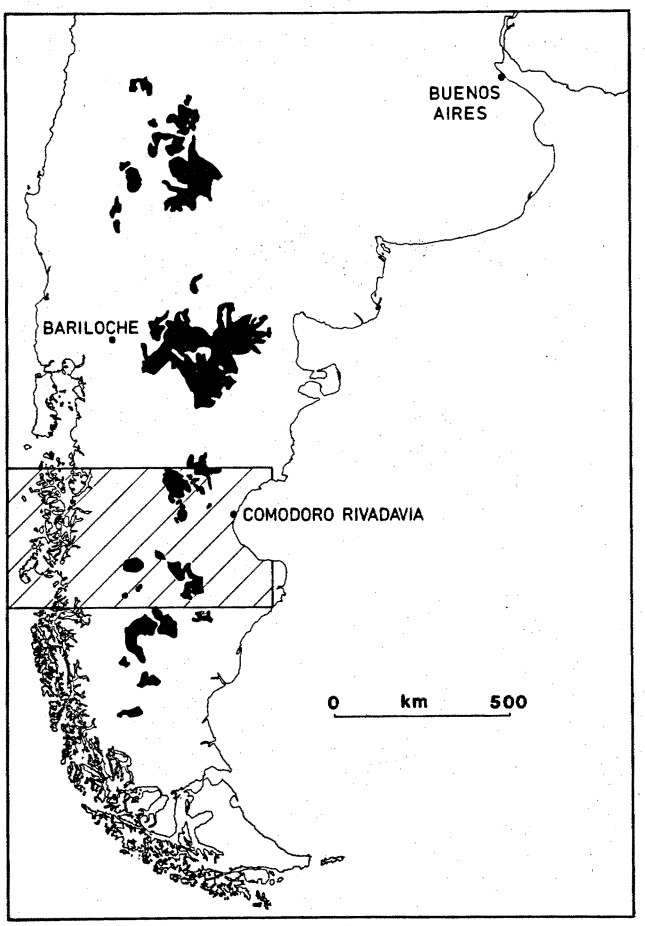

FIGURE 1. Location of area studied. Shaded areas indicate approximate distribution of plateau basalts (based on 1 :2 500 000 Mapa Geologico de la Republica Argentina 1964).

I. THE CORDILLERA

Figure 2 is a geological map of the area studied and also provides an index to the location of specimens collected by the expedition. Major- and trace-element analyses are presented in table 1; the igneous history of the area is described below.

MIDDLE TO UPPER JURASSIC VOLCANICS (IBAÑEZ FORMATION)

Field and petrographic relations

Volcanic rocks of Middle–Upper Jurassic age are abundant in the Patagonian Andes and are widely represented throughout much of the remainder of the Andean chain and Antarctic peninsula. In the area under consideration these volcanics (locally called the Elizalde and

Ibañez formations) lie in a nearly continuous belt running southwards from Coyhaique to Puerto Ibañez on the north side of Lago General Carrera. The volcanics were examined in two places: on the road running from Coyhaique westwards to Puerto Aisen where there is a succession of largely andesitic tuffs and volcaniclastics reaching a total thickness of 290 m (Skarmeta 1974); and in the area around Puerto Ibañez where a detailed collection was made.

In the area around Puerto Ibañez the Jurassic volcanics lie unconformably on Palaeozoic schists and phyllites and reach a total thickness of about 1000 m. The rocks have been uplifted and gently folded with generally north–south-trending fold axes. The volcanics include a wide variety of reworked pyroclastics as well as two distinct groups of primary volcanics: a group of basaltic andesite lava flows and a group of rhyolitic ash-flow tuffs.

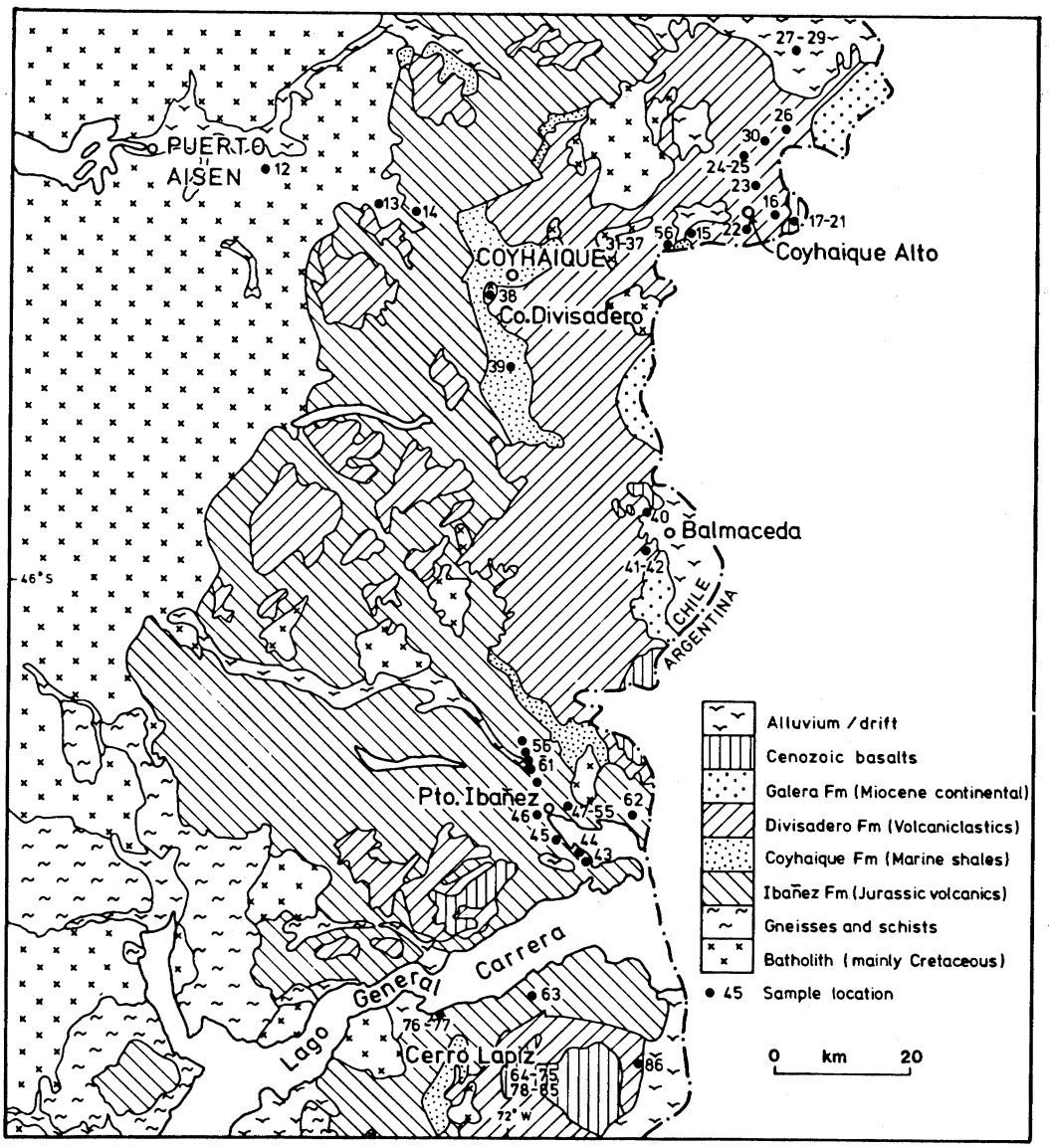

FIGURE 2. Simplified geological map of part of Aisen Province (after Skarmeta 1974) showing location of samples.

The lavas become more abundant towards the west of the area studied, i.e. towards the Patagonian batholith. They are porphyritic rocks containing phenocrysts of plagioclase (*ca.* 25 %†), altered mafic minerals (10–20 %), magnetite (less than 5 %), and sometimes quartz within fine grained pilotaxitic ground-masses. A few of the lavas contain amygdales of calcite and chlorite. All the lavas show the effects of lower greenschist facies metamorphism or hydrothermal alteration, or both, with plagioclase showing albitization and variable degrees of alteration to epidote or sericite. The original mafic minerals are more extensively altered, usually to aggregates of calcite and chlorite. In some samples (e.g. P53) the pseudomorph shapes suggest that the original mafic mineral was an amphibole but pyroxene was almost certainly more common in most rocks. One specimen (P57) contains recognizable pseudomorphs after olivine. Incipient cleavage is developed in a few specimens. Where alteration is less pronounced the rocks show petrographic features such as oscillatorily zoned plagioclases and corroded, embayed quartz crystals, which are typical of unaltered calc-alkaline andesites.

Interbedded with the andesitic lavas and apparently becoming more abundant towards the east and upwards in the Ibañez formation, are a series of rhyolitic ash-flow tuffs. The grain size of the ash flows varies, as does the relative proportion of crystal, lithic and vitric fragments. The crystal component (*ca.* 30 %) consists of strongly embayed and shattered quartz crystals; corroded plagioclase, partly altered to sericite, calcite and epidote; and potash feldspar and biotite altered to sericite and chlorite. The lithic component is particularly variable and includes fragments of older tuffs, andesite lavas and pumice which is slightly flattened in some specimens. Cuspate and tabular shards occur within the dusty matrices of the ash-flow tuffs. There is no evidence of welding in the specimens examined and in some instances delicate bubbles are preserved. The shards and bubble margins have largely divitrified to fine quartz-rich aggregate and in a few samples the entire original matrix has been overgrown by a quartzo–feldspathic aggregate. In the matrix of some samples (e.g. P50) there is patchy subparallel development of micaceous minerals indicating incipient cleavage development.

Chemistry, comparisons and petrogenesis

Chemical analyses of these rocks (table 1, nos 1–6) confirm the bimodal intermediate to acid character of the suite. The ash flow tuffs (table 1, nos 4–6) are rhyolitic with $SiO_2 > 70\,\%$‡. They have low TiO_2, high Al_2O_3 (all the analysed rocks contain some normative corundum), high K_2O and high K_2O/Na_2O ratios. Among the trace elements Rb, Sr and Zr are relatively high and Ba low compared with similar rocks from elsewhere (table 2, nos 7–10). Thus, compared with rhyolitic rocks of the same age from further south in the southern Andes (table 2, no. 7) and the Taupo rhyolites, New Zealand (table 2, no. 8) the rhyolites analysed here have less SiO_2 and Ba, lower K/Rb and Ba/Rb ratios, and more Al_2O_3, total iron, K_2O, Rb, Sr and Zr.

The intermediate lavas are basaltic andesites with $SiO_2 \approx 56\,\%$ and they have relatively low K, Rb and Ba. They show broad similarities to the average Patagonian batholith (table 2, no. 6) but are much richer in K_2O than the mafic lavas from the Upper Jurassic further south (table 2, no. 5).

The geochemical data presented here allow a preliminary assessment of the petrogenetic processes that gave rise to the volcanics and of the nature of the relation, if any, between the basaltic andesite lavas and the rhyolite ash-flow tuffs.

† Percentage mineral compositions are given by volume.
‡ Percentage chemical compositions are given by mass.

The lavas become more abundant towards the west of the area studied, i.e. towards the Patagonian batholith. They are porphyritic rocks containing phenocrysts of plagioclase (*ca.* 25 %†), altered mafic minerals (10–20 %), magnetite (less than 5 %), and sometimes quartz within fine grained pilotaxitic ground-masses. A few of the lavas contain amygdales of calcite and chlorite. All the lavas show the effects of lower greenschist facies metamorphism or hydrothermal alteration, or both, with plagioclase showing albitization and variable degrees of alteration to epidote or sericite. The original mafic minerals are more extensively altered, usually to aggregates of calcite and chlorite. In some samples (e.g. P53) the pseudomorph shapes suggest that the original mafic mineral was an amphibole but pyroxene was almost certainly more common in most rocks. One specimen (P57) contains recognizable pseudomorphs after olivine. Incipient cleavage is developed in a few specimens. Where alteration is less pronounced the rocks show petrographic features such as oscillatorily zoned plagioclases and corroded, embayed quartz crystals, which are typical of unaltered calc-alkaline andesites.

Interbedded with the andesitic lavas and apparently becoming more abundant towards the east and upwards in the Ibañez formation, are a series of rhyolitic ash-flow tuffs. The grain size of the ash flows varies, as does the relative proportion of crystal, lithic and vitric fragments. The crystal component (*ca.* 30 %) consists of strongly embayed and shattered quartz crystals; corroded plagioclase, partly altered to sericite, calcite and epidote; and potash feldspar and biotite altered to sericite and chlorite. The lithic component is particularly variable and includes fragments of older tuffs, andesite lavas and pumice which is slightly flattened in some specimens. Cuspate and tabular shards occur within the dusty matrices of the ash-flow tuffs. There is no evidence of welding in the specimens examined and in some instances delicate bubbles are preserved. The shards and bubble margins have largely divitrified to fine quartz-rich aggregate and in a few samples the entire original matrix has been overgrown by a quartzo–feldspathic aggregate. In the matrix of some samples (e.g. P50) there is patchy subparallel development of micaceous minerals indicating incipient cleavage development.

Chemistry, comparisons and petrogenesis

Chemical analyses of these rocks (table 1, nos 1–6) confirm the bimodal intermediate to acid character of the suite. The ash flow tuffs (table 1, nos 4–6) are rhyolitic with $SiO_2 > 70$ %‡. They have low TiO_2, high Al_2O_3 (all the analysed rocks contain some normative corundum), high K_2O and high K_2O/Na_2O ratios. Among the trace elements Rb, Sr and Zr are relatively high and Ba low compared with similar rocks from elsewhere (table 2, nos 7–10). Thus, compared with rhyolitic rocks of the same age from further south in the southern Andes (table 2, no. 7) and the Taupo rhyolites, New Zealand (table 2, no. 8) the rhyolites analysed here have less SiO_2 and Ba, lower K/Rb and Ba/Rb ratios, and more Al_2O_3, total iron, K_2O, Rb, Sr and Zr.

The intermediate lavas are basaltic andesites with $SiO_2 \approx 56$ % and they have relatively low K, Rb and Ba. They show broad similarities to the average Patagonian batholith (table 2, no. 6) but are much richer in K_2O than the mafic lavas from the Upper Jurassic further south (table 2, no. 5).

The geochemical data presented here allow a preliminary assessment of the petrogenetic processes that gave rise to the volcanics and of the nature of the relation, if any, between the basaltic andesite lavas and the rhyolite ash-flow tuffs.

† Percentage mineral compositions are given by volume.
‡ Percentage chemical compositions are given by mass.

Table 1 (*cont.*)

	(18)	(19)	(20)	(21)	(22)	(23)	(24)	(25)
SiO_2	64.6	58.9	58.7	61.7	55.9	68.3	46.1	48.0
TiO_2	0.59	0.67	0.68	0.70	0.99	0.27	1.35	0.75
Al_2O_3	15.2	16.9	17.0	16.2	18.0	15.7	17.1	18.7
Fe_2O_3	1.66	2.84	2.11	2.25	3.44	1.38	3.30	2.22
FeO	2.60	3.67	3.46	3.04	3.63	1.17	6.22	6.84
MnO	0.10	0.15	0.14	0.10	0.18	0.07	0.18	0.21
MgO	2.65	3.82	3.60	3.00	4.00	1.03	8.53	7.12
CaO	3.93	6.58	6.31	5.27	7.47	3.46	4.69	10.7
Na_2O	3.59	3.89	4.43	3.95	4.38	5.70	4.00	3.59
K_2O	2.37	1.51	2.26	2.00	1.23	1.07	1.32	0.65
P_2O_5	0.13	0.18	0.17	0.11	0.28	0.10	0.23	0.12
loss on ignition	—	—	1.98	2.15	—	—	—	0.20
total	—	—	100.84	100.47	—	—	—	99.10
			trace elements					
Rb	84	55	53	67	20	27	39	10
Sr	273	411	417	386	570	425	444	475
Ba	340	250	270	280	220	270	800	95
Zr	228	159	165	212	141	121	53	29
Nb	6	5	4	5	6	2	3	3
Y	37	27	30	31	28	15	29	24

Notes on table 1

Analysts

R. Fuge, H. Edwards, G. Lees.

Methods

SiO_2, Al_2O_3, TiO_2, P_2O_5, Fe_2O_3, automated photometry; MgO, CaO, MnO, atomic absorption; Na_2O, K_2O, flame emission; FeO, dichromate; Rb, Sr, Ba, Zr, Nb, Y, X.R.F. spectroscopy.

The X.R.F. analyses were done at the Geology Department, University of Keele. Spiked internal laboratory standards olivine basanite (KU1–2) and granite porphyry (KU1) were used for calibration of the basic and intermediate to acid rocks respectively. The internal standards have overall a similar mineralogy to the analysed rocks. Accuracy was checked by using international standards W-1, BCR-1(2), BR, JB-1, AGV-1, GSP-1, G-2(1), GA and GH, all of which gave acceptable results when compared with recommended values quoted by Abbey (1978).

Details of analysed specimens (locations given on figure 2)

(1) P51 Andesite lava. Phenocrysts of plagioclase (altered to epidote) and (?) pyroxene (altered to chlorite–calcite aggregates). Ibañez Formation. East of Puerto Ibañez, Chile.

(2) P53 Andesite lava. Phenocrysts of plagioclase (altered to calcite, sericite and epidote) and (?) pyroxene (altered to chlorite–calcite aggregates). Ibañez Formation. East of Puerto Ibañez, Chile.

(3) P60 Andesite lava. Phenocrysts of plagioclase (altered to sericite, calcite and rare epidote) and (?) pyroxene (altered to chlorite–calcite aggregates) in a fine plagioclase-rich matrix. Ibañez Formation. North of Puerto Ibañez, Chile.

(4) P50 Rhyolite ash flow tuff. Fragments of crystals (quartz, plagioclase, potash feldspar, biotite), lithics, slightly flattened pumice. Matrix obscured by secondary overgrowth and incipient cleavage development, but small cuspate shards are present. Ibañez Formation. East of Puerto Ibañez, Chile.

(5) P56 Rhyolite ash flow tuff. Lithic (20%) and crystal (10%–mainly plagioclase and quartz fragments in a recrystallized quartzitic matrix. Remnants of flattened pumice. Ibañez Formation. North of Puerto Ibañez, Chile.

(6) P59 Rhyolite ash flow tuff. Crystal and lithic fragments. Very fine and partly recrystallized shardic matrix. Ibañez Formation. North of Puerto Ibañez, Chile.

(7) P61 Plagioclase–hornblende microdiorite. Small intrusion into Ibañez Formation. North of Puerto Ibañez, Chile.

(8) P12 Biotite–hornblende granite (grey granite), Patagonian batholith. Road from Coyhaique to Puerto Aisen, Chile.

(9) P13 Granophyric leucogranite (pink granite), Patagonian batholith. Road from Coyhaique to Puerto Aisen, Chile.

PHILOSOPHICAL TRANSACTIONS OF THE ROYAL SOCIETY A MATHEMATICAL, PHYSICAL & ENGINEERING SCIENCES

Table 1 (*cont.*)

	(18)	(19)	(20)	(21)	(22)	(23)	(24)	(25)
SiO_2	64.6	58.9	58.7	61.7	55.9	68.3	46.1	48.0
TiO_2	0.59	0.67	0.68	0.70	0.99	0.27	1.35	0.75
Al_2O_3	15.2	16.9	17.0	16.2	18.0	15.7	17.1	18.7
Fe_2O_3	1.66	2.84	2.11	2.25	3.44	1.38	3.30	2.22
FeO	2.60	3.67	3.46	3.04	3.63	1.17	6.22	6.84
MnO	0.10	0.15	0.14	0.10	0.18	0.07	0.18	0.21
MgO	2.65	3.82	3.60	3.00	4.00	1.03	8.53	7.12
CaO	3.93	6.58	6.31	5.27	7.47	3.46	4.69	10.7
Na_2O	3.59	3.89	4.43	3.95	4.38	5.70	4.00	3.59
K_2O	2.37	1.51	2.26	2.00	1.23	1.07	1.32	0.65
P_2O_5	0.13	0.18	0.17	0.11	0.28	0.10	0.23	0.12
loss on ignition	—	—	1.98	2.15	—	—	—	0.20
total	—	—	100.84	100.47	—	—	—	99.10
			trace elements					
Rb	84	55	53	67	20	27	39	10
Sr	273	411	417	386	570	425	444	475
Ba	340	250	270	280	220	270	800	95
Zr	228	159	165	212	141	121	53	29
Nb	6	5	4	5	6	2	3	3
Y	37	27	30	31	28	15	29	24

Notes on table 1

Analysts

R. Fuge, H. Edwards, G. Lees.

Methods

SiO_2, Al_2O_3, TiO_2, P_2O_5, Fe_2O_3, automated photometry; MgO, CaO, MnO, atomic absorption; Na_2O, K_2O, flame emission; FeO, dichromate; Rb, Sr, Ba, Zr, Nb, Y, X.R.F. spectroscopy.

The X.R.F. analyses were done at the Geology Department, University of Keele. Spiked internal laboratory standards olivine basanite (KU1–2) and granite porphyry (KU1) were used for calibration of the basic and intermediate to acid rocks respectively. The internal standards have overall a similar mineralogy to the analysed rocks. Accuracy was checked by using international standards W-1, BCR-1(2), BR, JB-1, AGV-1, GSP-1, G-2(1), GA and GH, all of which gave acceptable results when compared with recommended values quoted by Abbey (1978).

Details of analysed specimens (locations given on figure 2)

(1) P51 Andesite lava. Phenocrysts of plagioclase (altered to epidote) and (?) pyroxene (altered to chlorite–calcite aggregates). Ibañez Formation. East of Puerto Ibañez, Chile.

(2) P53 Andesite lava. Phenocrysts of plagioclase (altered to calcite, sericite and epidote) and (?) pyroxene (altered to chlorite–calcite aggregates). Ibañez Formation. East of Puerto Ibañez, Chile.

(3) P60 Andesite lava. Phenocrysts of plagioclase (altered to sericite, calcite and rare epidote) and (?) pyroxene (altered to chlorite–calcite aggregates) in a fine plagioclase-rich matrix. Ibañez Formation. North of Puerto Ibañez, Chile.

(4) P50 Rhyolite ash flow tuff. Fragments of crystals (quartz, plagioclase, potash feldspar, biotite), lithics, slightly flattened pumice. Matrix obscured by secondary overgrowth and incipient cleavage development, but small cuspate shards are present. Ibañez Formation. East of Puerto Ibañez, Chile.

(5) P56 Rhyolite ash flow tuff. Lithic (20%) and crystal (10%–mainly plagioclase and quartz fragments in a recrystallized quartzitic matrix. Remnants of flattened pumice. Ibañez Formation. North of Puerto Ibañez, Chile.

(6) P59 Rhyolite ash flow tuff. Crystal and lithic fragments. Very fine and partly recrystallized shardic matrix. Ibañez Formation. North of Puerto Ibañez, Chile.

(7) P61 Plagioclase–hornblende microdiorite. Small intrusion into Ibañez Formation. North of Puerto Ibañez, Chile.

(8) P12 Biotite–hornblende granite (grey granite), Patagonian batholith. Road from Coyhaique to Puerto Aisen, Chile.

(9) P13 Granophyric leucogranite (pink granite), Patagonian batholith. Road from Coyhaique to Puerto Aisen, Chile.

PHILOSOPHICAL TRANSACTIONS OF THE ROYAL SOCIETY A MATHEMATICAL, PHYSICAL & ENGINEERING SCIENCES

Partial melting in the upper mantle above the subduction zone might also play a role in the genesis of Andean andesites. Water-rich fluids rising from the descending slab into the upper mantle will lower the solidus temperature and may induce melting. However, certain problems exist with regard to this process. For example, melting at the water concentrations required to bring about adequate lowering of the solidus temperature may produce magma more siliceous

TABLE 2. AVERAGE AND COMPARATIVE ANALYSES FOR CORDILLERAN ROCKS

(Data are given for major elements as % by mass; for trace elements in μg/g.)

	(1)	(2)	(3)	(4)	(5)	(6)	(7)	(8)	(9)	(10)
SiO_2	56.6	71.5	74.9	62.2	54.4	60.0	77.4	75.3	73.2	76.0
TiO_2	0.84	0.21	0.19	0.62	0.94	0.61	0.13	0.27	0.24	0.13
Al_2O_3	16.9	14.8	12.7	16.3	17.7	17.4	12.1	13.5	13.4	12.2
Fe_2O_3	2.51	1.97	1.05	2.35	7.81	6.20	1.37	1.68	2.23	1.70
FeO	4.62	1.32	0.26	2.58						
MgO	3.23	0.88	0.47	2.74	6.02	3.23	1.12	0.25	0.44	0.12
CaO	5.35	1.97	1.00	5.08	6.87	5.94	0.67	1.49	2.07	0.82
Na_2O	5.29	3.60	2.95	4.38	4.87	3.45	2.69	4.12	3.75	4.02
K_2O	1.14	3.82	4.90	1.99	0.30	1.66	3.53	3.39	3.38	3.97
P_2O_5	0.30	0.05	0.06	0.16	0.26	0.16	0.03	—	0.06	0.03
Rb	44	195	144	58	—	57	117	108	123	162
Sr	623	247	126	398	400	326	126	125	193	41
Ba	190	617	623	310	—	484	872	870	812	334
Zr	154	205	125	188	134	92	159	160	146	196
Nb	12	15	11	5	7	13	12	6	20	30
Y	32	39	29	30	42	—	—	—	—	—

(1) Average Jurassic andesite (table 1 nos 1–3).
(2) Average Jurassic rhyolite (table 1 nos 4–6).
(3) Average Cretaceous–Tertiary rhyolite (table 1 nos 10–16).
(4) Average intrusion into Cretaceous–Tertiary volcanics (table 1 nos 17–24).
(5) Mafic lavas within Tobifera, north of Beagle Canal, Argentina (Bruhn *et al.* 1978).
(6) Average Patagonian batholith – volumetrically weighted, average between 51 and 52°S (Stern & Stroup 1980).
(7) Average rhyolite from Tobifera, southernmost Andes (Bruhn *et al.* 1978).
(8) Average silicic volcanic, Taupo, New Zealand (Ewart *et al.* 1968).
(9) Average Patagonian batholith with $72 \leqslant SiO_2 \leqslant 75\%$ (Stern & Stroup 1980).
(10) Average Patagonian batholith with $SiO_2 > 75\%$ (Stern & Stroup 1980).

In analyses (5)–(10) total iron is given as FeO.

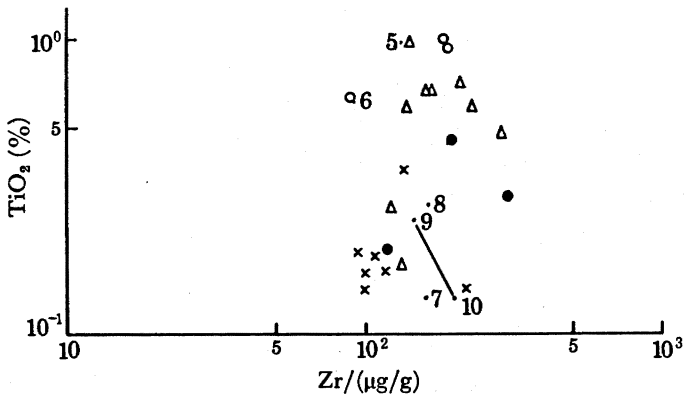

FIGURE 3. Plot of TiO_2 against Zr for cordilleran rocks. Jurassic volcanics: ○, basaltic andesite; ●, rhyolite. ×, Cretaceous–Tertiary (Divisadero) volcanics; △. intrusions (these are mainly intrusions into the Divisadero but include one analysis of the batholith and one of an intrusion into the Jurassic). Numbers refer to average analyses given in table 2.

than the basaltic andesites under discussion (Kushiro 1969). There is also the problem of the ascent of the presumably water-rich magma produced in this way, as studies have shown that water-saturated magmas, even when they ascend adiabatically, will solidify at great depth (Harris 1977). A further difficulty concerns the enrichment in alkaline elements in the basaltic andesites compared with the source peridotite, a problem that is even greater than that which exists for an oceanic tholeiite source. For example, K_2O in the basaltic andesites, considered here, is about 1.1 % compared with about 0.025 % in peridotite and 0.25 % in oceanic tholeiite. Interestingly, the basaltic andesites show strong enrichment in K and Rb compared with Nb, Zr, Ti and P (figure 4), and one possible way in which such a pattern might be developed is through the preferential incorporation of the former elements into an aqueous phase generated by dehydration of the subducted slab (Hawkesworth *et al.* 1979).

Contamination of mantle-derived melts within the crust above subduction zones has been invoked to account for certain characteristics, especially relatively high initial $^{87}Sr/^{86}Sr$ ratios, in some andesites. However, relatively high ratios may be generated within the upper mantle (Kramers 1977) or within oceanic crust through interaction with sea water (Hawkesworth *et al.* 1977) so that occurrences of relatively high radiogenic strontium in andesites can be reconciled

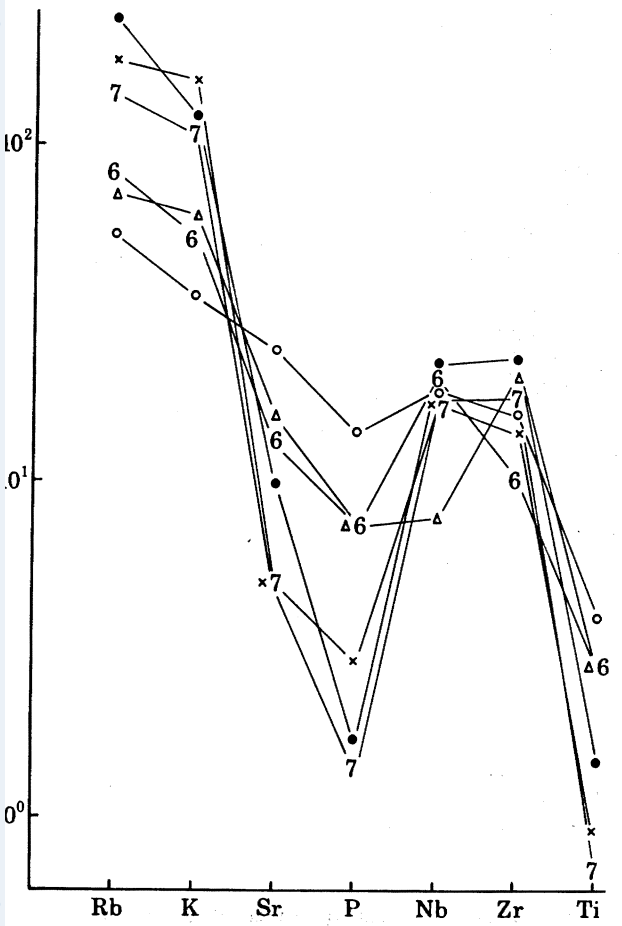

FIGURE 4. Mantle-normalized trace-element distribution patterns for igneous rocks of Aisen Province. Symbols are as in figure 3.

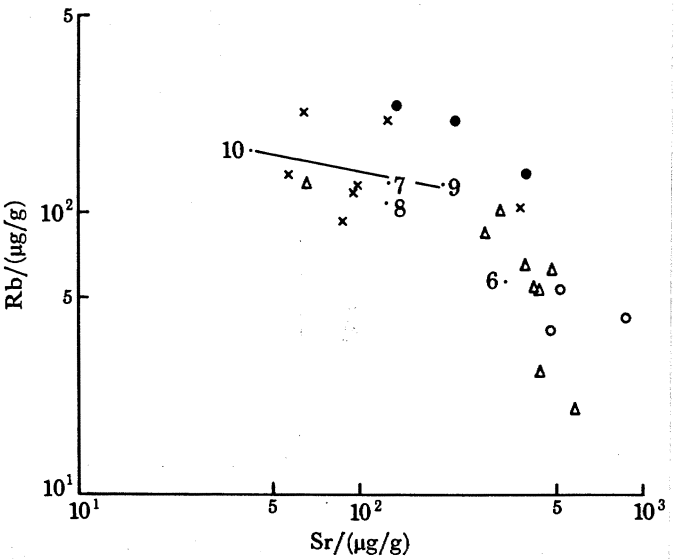

FIGURE 5. Plot of Rb against Sr for igneous rocks of Aisen Province. Symbols are as in figure 3.

with an origin by partial melting of either oceanic tholeiite or mantle peridotite, thereby eliminating the need to invoke crustal contamination.

Fractionation might, however, be more important and would probably involve early separation of olivine and pyroxene or chrome spinel to reduce Ni and Cr to values characteristic of andesite. Such fractionation must be particularly important if the primary source of the andesites is mantle peridotite. However, there is no direct evidence of deep-level fractionation in that there is no olivine- or Cr-rich phase or indeed any high pressure mineral in the basaltic andesites. The minerals present generally indicate growth at relatively shallow depths, normally of around 10 km or less. Of the minerals present in the andesites, fractionation of plagioclase may be important in controlling rare-earth-element distribution as is the case elsewhere in the Andes (Thorpe *et al.* 1976). Other phases that might be involved include orthopyroxene, magnetite and amphibole, but phases like biotite, zircon and apatite are unlikely to be involved at the relatively low SiO_2 contents under discussion here. Fractionation might proceed in closed systems but open-system fractionation (O'Hara 1977) is likely to be particularly effective in producing certain of the observed chemical characteristics, particularly the increase in compatible elements.

To summarize, the basaltic andesites are thought to have originated in response to easterly subduction of oceanic crust along the western margin of Gondwanaland. Partial melting of subducted oceanic tholeiite is thought to be more important than wet partial melting of mantle peridotite above the subduction zone, and in the subsequent modification of the original magmas fractionation, especially open system fractionation, is likely to be more significant than crustal contamination.

Apart from the origin of the basaltic andesites the other major petrogenetic problem concerns the relation of the basaltic andesites to the rhyolites. As stated, the two are intimately associated in the field being contemporaneous and interbedded with one another but there is a large compositional gap between the two groups. Such bimodal volcanism has been common at different times in many parts of the Andes, and authors are divided on the question of the relation between the two groups. Some (e.g. Bruhn *et al.* 1978, Pichler & Zeil 1972) consider the acid rocks to be the result of crustal fusion, heat for which is provided by rising basic magma or by rising mantle diapirs (Oxburgh & Parmentier 1977), a mechanism that is also capable of producing vertical tectonics and initiating back-arc spreading. Others (e.g. Thorpe & Francis 1979) regard the acid rocks as fractionation products from the more basic magmas.

Supporters of a fractionation relation between rhyolites and andesites elsewhere invoke early fractionation of mafic minerals (pyroxene, amphibole) and plagioclase, with later fractionation dominated by plagioclase (Thorpe *et al.* 1979). Plagioclase-dominated fractionation at depths below 35 km will account for the increase in Rb and decrease in Sr in the rhyolites shown in figure 5. However, plagioclase fractionation would also be expected to result in a decrease in Ba/Rb with increasing SiO_2, which is the reverse of the trend observed here. In addition, plagioclase-dominated fractionation would not account for the sharp decrease in TiO_2 seen in the most acid of the rhyolites. It is clear from this discussion that most chemical characteristics of the rhyolites require fractionation of other phases in addition to plagioclase but this considerably increases the amount of fractionation required to give the observed Rb/Sr variation.

Some of the geochemical evidence is compatible with an origin for the rhyolites by crustal melting. Thus the rhyolites plot within the field of crustal melts on a Nb–SiO_2 diagram (Pearce & Gale 1977). The rhyolites also show close geochemical similarities to rhyolites from further

PHILOSOPHICAL TRANSACTIONS OF THE ROYAL SOCIETY A MATHEMATICAL, PHYSICAL & ENGINEERING SCIENCES

south in the Andes (Bruhn *et al.* 1978) and to the Taupo volcanics, New Zealand (Ewart *et al.* 1968), for both of which an anatectic origin has been proposed. There are, however, certain problems in deriving the Jurassic rhyolites, described here, by crustal melting. For example, no recognizable xenoliths of lower crustal material occur within the thyolites, and also the Jurassic crust was probably too thin for melting to have occurred. The present crustal thickness of about 30 km (Cummings & Schiller 1971) includes major post-Jurassic increments.

Regional considerations also have a bearing on the origin of these rocks. The Middle–Upper Jurassic rocks described here belong to a group (often referred to informally as the Tobifera) that is very abundant in the Patagonian Andes, at least southwards from about 40 °S, and that is widely represented throughout much of the remainder of the Andean chain and Antarctic peninsula. In South America these rocks occur within a volcano–tectonic rift zone stretching from 40–54 °S and from approximately 72 °W to at least 66 °W (Bruhn *et al.* 1978). An eastward extension of the province is suggested by the interpretation of seismic refraction profiles of the Atlantic continental shelf east of Patagonia (Ludwig *et al.* 1968). The dominant volcanics in this series are silicic ignimbrites but mafic lavas are interbedded in places, and intermediate lavas in others (Bruhn *et al.* 1978). It is clear from the foregoing that there is, within this province, a great volume of rhyolite and that there are also substantial compositional gaps in the volcanic series. These gaps are different in different places, for example, being from basalt to rhyolite in the southernmost Andes (Bruhn *et al.* 1978) and from basaltic andesite to rhyolite in the area discussed here.

It is possible that, in the west, the intrusive rocks of the Patagonian batholith, which are of overall intermediate composition (table 2, no. 6), fill the compositional gap to give an essentially fractionation-related sequence of rocks, but there is no evidence for the existence of the batholith in the east. In addition, although initial $^{87}Sr/^{86}Sr$ ratios in the rhyolites and the batholith are identical, chemical trends are different. In the batholith Rb, Zr, Nb and Rb/Sr increase and Sr, Ba, K/Rb and Ba/Rb decrease with increasing SiO_2, whereas the rhyolites show trends towards higher Sr, Ba and Ba/Rb and lower Rb, Zr and Rb/Sr with increasing SiO_2.

On this evidence the fractionation hypothesis for the andesites is hard to sustain and an origin by crustal fusion seems more likely. The overall tectonic petrogenetic setting at this stage is, therefore, thought to have been a volcanic arc in the west, with andesites and their plutonic equivalents, the early stages of the Patagonian batholith, being produced in response to easterly subduction along the western margin of Gondwanaland. To the east of this volcanic arc was a large volcano–tectonic depression characterized by mildly extensional tectonics and abundant rhyolites with subordinate basalts and trachytes. Rhyolites also occur within the volcanic arc where they are intimately associated with calc-alkaline volcanics. In both situations the rhyolites are thought to form by crustal melting. Volume relations and major-element geochemistry are consistent with an origin for the western rhyolites by fractional crystallization from the calc-alkaline andesites, but trace-element variation fails to support such an origin. In the east, the vast quantities of rhyolitic material together with the paucity or total absence of intermediate material make an origin by fractional crystallization even less likely.

Lower Cretaceous sediments (Coyhaique Formation)

The Neocomian rocks of the Aisen province of Chile have been described and their tectonic significance has been discussed by Skarmeta (1976) In the investigation described here

observation of the Neocomian rocks was restricted to the area around Coyhaique where there are few igneous rocks present so that the following account is taken largely from Skarmeta's work.

In the Coyhaique area, the Jurassic volcanics and volcaniclastics (Elizalde Formation) become more arenaceous upwards and pass conformably into a group (Coyhaique Formation), composed of marine sediments, which are arenaceous at the base and become generally finer upwards. Slightly to the west of this marine sedimentary succession, for example, at Rio Emperador Guillermo, the shales and sandstones are intercalated with andesitic tuffs, which Skarmeta (1976) believes to be derived from an island arc to the west. The site of the island arc is now marked not by volcanics but by the Patagonian batholith, which presumably represented the roots of the arc. Still further to the west in Isla Traiguen more basic to andesitic volcanics were interbedded with open-sea sediments.

The inferred tectonic reconstruction from west to east is thus from arc-trench gap through island arc into a marine back-arc basin. In the Coyhaique area, the depth of the basin as inferred from sedimentary or palaeontological evidence was probably quite limited, and the restricted lateral extent of the Neocomian sediments suggests that the basin was narrow but opening to the south. Some evidence of extension is provided by the basic dykes that cut the Neocomian sediments. The tectonic situation implied here is similar to that inferred for the Upper Jurassic, i.e. a volcanic arc to the west with an extensional basin to the east. In the Lower Cretaceous, however, greater extension and depression of the area behind the arc occurred creating a marine back-arc basin, and the voluminous rhyolitic volcanism that characterized the Upper Jurassic ceased.

Comparisons can also be made with the Lower Cretaceous rocks about 700 km to the south where Dalziel *et al.* (1974) and Bruhn *et al.* (1978) have described two ophiolites believed to have formed by sea-floor spreading within a marginal basin. The opening of this back-arc basin probably took place in earliest Cretaceous times, separating a sliver of Palaeozoic basement from the remainder of the continent. A volcanic island arc was situated along this severed strip, and the development of the Patagonian batholith took place beneath the arc. The basin was partially filled by Lower Cretaceous sediments and closed again during the mid-Cretaceous. Although the overall picture of a marine basin bordered to the west by an island arc is the same in both areas there are certain significant differences. The basin was narrower and shallower in the Coyhaique area, the sediments are fine-grained shales rather than flysch deposits and the amount of igneous activity within the basin was much more limited, being apparently confined to the injection of a few dykes. Again in contrast to the area to the south, the eventual closure of the basin resulted neither in the emplacement of ophiolites nor in the development of penetrative tectonic fabrics. It is as if the basin was eliminated simply by filling or by marine regression. Uplift may have been important in the elimination of the basin either by lifting the level of the basin or by raising the level of the sediment source area and thus increasing the supply of sediment, but there seems to have been little horizontal movement.

Middle Cretaceous–(?) Lower Tertiary volcanics (Divisadero Formation)

Rocks of Middle Cretaceous age (Divisadero Formation (Skarmeta 1974)) overlie the rocks of the Coyhaique Formation. The contact is gradational and marks a change from marine to fluviatile–lacustrine conditions. It is apparent, however, that the base of the Divisadero

Formation becomes consistently younger towards the south giving ages progressively younger southwards for the closure of the Neocomian marine basin.

It is probable that the top of the Divisadero Formation is also diachronous. Ages of the plateau basalts immediately overlying the Divisadero Formation range from almost 80 Ma (Morro Negro, Senguerr) to about 20 Ma (Perito Moreno), and in places rocks of the Galera Formation (probably Oligocene to Miocene) appear to overlie conformably rocks belonging to the Divisadero Formation.

The rocks of the Divisadero Formation include tuffs, lavas and a large amount of volcaniclastics. There are more lava flows in the west and a higher proportion of pyroclastics and volcaniclastics in the east. The relative proportion of volcaniclastic to primary volcanic material also increases upwards and some of the upper deposits contain clasts of pink orthoclase, quartz with undulose extinction and myrmekite, suggesting derivation from a granitic terrain. The total thickness of the Divisadero Formation is almost 1000 m.

There is a general tendency for the rocks to become more acid upwards, and in the uppermost parts of the formation, from which the analysed volcanics were collected, most of the primary volcanics are rhyolitic with both lavas and ash-flow tuffs represented. In both cases phenocrysts of biotite, plagioclase, orthoclase and embayed quartz occur but the ash-flow tuffs contain glass shards and flattened tubular pumice fragments whereas the lavas have microcrystalline groundmasses.

The compositions of lavas (table 1, nos 10, 13) ash-flow tuffs (table 1, nos 11, 14–16) and of high level intrusions into the volcanics (table 1, no. 12) are very similar which suggests that the last mentioned were feeders for the volcanics. These rhyolites are generally similar in composition to the Upper Jurassic rhyolites but are richer in SiO_2 and K_2O, poorer in Al_2O_3, total iron, MgO, CaO, Na_2O, Rb, Sr and Zr, and have higher K/Rb and Rb/Sr ratios. They are richer in SiO_2 and K_2O than the rhyolites described by Bruhn *et al.* (1978) and are higher in K_2O, Rb and lower in Na_2O than the Taupo volcanics. Plotted on a Ti–Zr diagram (figure 3) these rocks plot well within the calc-alkaline field. Thorpe & Francis (1979) have described a general westward increase in K, Rb and, to a lesser extent, SiO_2 in younger Andean rocks but such trends are not apparent from the admittedly limited data presented here. Indeed there is a surprising uniformity in composition of these rhyolites which may be of different ages but which everywhere immediately underlie the Patagonian plateau basalts.

The Divisadero Formation appears to be almost entirely subaerial. Indeed the boundary with the underlying Neocomian is taken at the transition between submarine and subaerial deposits. The tectonic environment within which the formation developed is that of an active continental margin, although some of the rhyolites probably developed in a tensional environment behind the main axis of volcanism. There is some evidence from detailed mapping (Skarmeta 1974) that the main axis of volcanic activity shifted eastwards towards the end of Divisadero times. Beneath the volcanics intrusive activity continued within the Patagonian batholith, which formed the roots of the volcanic chain. Towards the end of the period, however, the batholith was clearly exposed to erosion in the west as Divisadero sediments derived from the east contain fragments derived from a batholith source. It seems likely, therefore, that a period of uplift occurred towards the end of Divisadero times and this would have eliminated the small basins that formed the remnants of the Neocomian sea. The uplift might also have been associated with the period of lower greenschist facies metamorphism which has affected some of the igneous rocks in the area.

PHILOSOPHICAL TRANSACTIONS OF THE ROYAL SOCIETY A MATHEMATICAL, PHYSICAL & ENGINEERING SCIENCES

The overall tectonic picture for Divisadero times differs from that existing in the Neocomian inasmuch as the volcanic arc is then non-marine with the major axis displaced slightly to the east, and the back-arc environment is subaerial rather than submarine. The situation is thus much closer to that existing in the Middle–Upper Jurassic, and the petrogenetic problems, especially the origin of the voluminous rhyolites and the nature of the relation between the rhyolites and the batholith and other intrusions, are also similar.

Compared with the Jurassic rhyolites, the Divisadero rhyolites are probably less voluminous and appear to extend less far to the east. They also show certain chemical trends, e.g. decrease in Ba/Rb with increasing SiO_2, that are more compatible with plagioclase-controlled fractionation. Again the associated minor intrusions of intermediate to acid composition (table 1, nos 17–23) form almost continuous chemical trends with the rhyolites in many chemical parameters, e.g. Rb and Sr (figure 4). It is possible therefore that some of these rhyolites, especially those in the west, represent the end products of fractionation from magmas generated in response to subduction along the Pacific coast of South America. As one moves eastwards, however, the proportion of rhyolite appears to increase, and the number of intrusive bodies decreases so that here an origin for the rhyolites by fractionation is less likely.

The relation of the rhyolites to the plateau basalts that overlie them in many places may be relevant to the question of the origin of the rhyolites. This relation is not completely understood but the fact that both the rhyolitic rocks and the early basalt lavas, which tend to be tholeiitic, may have formed by fissure eruption in a tensional environment may be significant. It is also possible that the thermal activity that eventually produced the basalts by melting within the upper mantle first gave rise to melting at the base of the crust to produce the rhyolites.

There may thus be a distinction between the tectonic and petrogenetic situation as one goes from west to east. In the west within an active continental margin, rooted by the Patagonian batholith, petrogenesis may have been related primarily to subduction with fractionation giving rise to some of the rhyolites. In the east, behind the arc, where activity is more predominantly rhyolitic and where there is an absence of batholith and other intermediate intrusive activity, an origin for the rhyolites by crustal melting related to the rising mantle diapir that ultimately produced the Patagonian basalts is more likely.

Intrusions

The Patagonian batholith

The Patagonian batholith was studied briefly in the area between Coyhaique and Aisen. Here an older pink granite (table 1, no. 9), which predates the upper part of Coyhaique Formation and which contributed clasts to the Divisadero Formation, is cut by a grey granite (table 1, no. 8) which also cuts the lower part of the Divisadero Formation. There is some difference in composition between the two granites: the early pink granite is richer in silica, it is peralkaline and has a distinctly granophyric texture. A K–Ar age determination on the grey granite gave a value of 97 Ma which is in keeping with the Upper Cretaceous age suggested by the stratigraphic relations.

Halpern & Fuenzalida (1978) have recently published Rb–Sr ages for a transect of the Chilean Andes between 45 and 46 °S i.e. in the area around Coyhaique. These ages range from 176 to 12 Ma in rocks ranging in composition from quartz diorite to adamellite. The ages do not

show any simple unidirectional migration and there is no evidence of the post-Palaeozoic eastward migration of plutonic foci found in the central Andes (Farrar *et al.* 1970).

Halpern & Fuenzalida's dates between 45 and 46 °S are similar to those from the batholith elsewhere in the southern Andes. In the Argentine Andes between 40 and 44 °S (Toubes & Spikermann 1973, Halpern *et al.* 1975) ages range from late Palaeozoic (350 Ma) to Cretaceous (84 Ma) while further south in Chile, in the Magellanes province near Puerto Natales, Halpern (1973) has obtained ages ranging from Upper Jurassic to late Tertiary with concentrations of intrusives around 130 Ma and 90 Ma.

Dalziel *et al.* (1974) and Bruhn *et al.* (1978) consider that in the Puerto Natales region the Patagonian batholith represented the roots of an active calc-alkaline volcanic belt. A similar situation is thought to have existed in Aisen. At this stage it is not possible to correlate exactly periods of plutonic and volcanic activity, and activity may be virtually continuous if the batholith is considered as a whole. However, it is possible that the local concentrations of ages reported by Halpern & Fuenzalida in the Coyhaique area of between 100 and 110 Ma might correspond to the beginning of Divisadero activity.

Another interesting inference from Halpern & Fuenzalida's work is that the initial Sr isotope ratios that they report at around 0.7045 must imply limited involvement of old continental material in the genesis of these rocks. This would tend to confirm an origin related to subduction either through wet mantle melting (cf. Brown 1977) or through partial melting of subducted oceanic tholeiite. For reasons given earlier the latter process is thought to be more important.

Other intrusions

Minor intrusions cut the rocks of the Divisadero Formation. These intrusions cover a wide range in composition from basic to acid (table 1, nos 18–24). It is probable that many of the intrusions acted as feeders for the Divisadero volcanics. Basic volcanics do not, however, occur within the Divisadero Formation so that the olivine tholeiite intrusions (e.g. table 1, no. 24) are probably related to an early phase of the plateau basalt activity.

Clearly, on account of their age relations, association with the Divisadero volcanics and general composition, many of these intrusions belong to the same general period of activity as the Patagonian batholith and might best be regarded as outliers of the batholith. Like the batholith they may also have been emplaced over a period of time. Thus, although they are all post-Divisadero in age, some of the intrusions show evidence of having experienced a period of lower greenschist facies regional metamorphism or hydrothermal alteration whereas others are fresh and may thus post-date the alteration episode.

As stated earlier the intrusions may, in many cases, have acted as feeders for the Divisadero volcanics. None of the intrusions, however, is as acid as the Divisadero rhyolites so that the possibility remains that the Divisadero rhyolites have originated from a separate source.

Post-Divisadero geological history

The geological history of the area in the period following the deposition of the Divisadero Formation is complex and there is evidence to suggest that Divisadero activity continued later in some areas than in others. In a few places the presence of richly fossiliferous sandstones is evidence of an Upper Cretaceous–Palaeocene marine transgression of the Atlantic (Charrier *et al.* 1978).

PHILOSOPHICAL TRANSACTIONS OF THE ROYAL SOCIETY A MATHEMATICAL, PHYSICAL & ENGINEERING SCIENCES

Elsewhere the rocks of the Divisadero Formation are in contact with the Patagonian plateau basalts or with rocks assigned either to the Guadal or the Galera Formations (Skarmeta 1978). The Guadal Formation is of possible Upper Eocene–Lower Oligocene age and at least partly marine. Where the Guadal sediments are thickest and show the clearest evidence of submarine deposition, the Patagonian basalts are also thickest. This suggests that where subsidence was greatest, the subsequent volume of basalt magmatism was also greatest.

Where rocks of the Divisadero Formation are overlain by rocks of the Galera Formation, which is probably of Oligocene–Miocene age, the contact is occasionally conformable but is usually an unconformity with evidence that a period of uplift has occurred. The Galera Formation consists of rapidly deposited clastic sediments of fluviatile origin, which were transported by rivers flowing eastwards off the Andean cordillera.

Calc-alkaline volcanic activity in the area studied appears therefore to end with the Divisadero Formation. However, in the cordillera to the west (Cerro Hudson) and north (for example, Volcan Atillanca, table 1, no. 25) calc-alkaline activity has continued to the present day. In addition Halpern & Fuenzalida's (1978) data suggest that activity within the Patagonian batholith may also have continued up until at least Miocene times. In the area described here the next volcanic event was the eruption of the Patagonian plateau basalts.

Summary and discussion

The igneous history of the area under discussion is essentially the history of a volcanic–batholith arc in the west and a back-arc basin to the east. The probable existence of a subduction system in Upper Palaeozoic times is suggested by the presence of a tectonic melange and blueschist facies metamorphism in the Upper Palaeozoic rock record (Gonzalez & Aguirre 1968), and from the thermal–plutonic activity in eastern Patagonia (de Wit 1977). However, the first evidence of the system presented here is in rocks of Middle–Upper Jurassic age where the arc activity consists of calc-alkaline volcanics and plutonics with voluminous, mainly rhyolitic, subaerial volcanism characterizing the back-arc area. Towards the end of the Jurassic the western arc separated from the South American continent, and the back-arc basin became marine. Extension within the back-arc basin, as indicated by the presence of basaltic dykes, was fairly limited and the basin was filled largely by fine-grained sediments of Lower Cretaceous age. The marine basin was eliminated by Middle Cretaceous times by vertical uplift rather than by horizontal closure. The elimination of the basin involved no development of penetrative tectonic fabrics, and in many places there is no unconformity between the Lower Cretaceous sediments and the succeeding Middle Cretaceous volcanics. The Middle Cretaceous situation was apparently similar to that existing in the Middle Jurassic, i.e. a continental arc with calc-alkaline igneous activity in the west and more rhyolitic activity behind the arc towards the east. As in the Upper Jurassic the rhyolite activity was followed by a marine transgression although in this case the effects of the transgression (Guadal Formation) were more restricted and faunal evidence shows that the transgression was from the Atlantic rather than the Pacific. Again, as in the Upper Jurassic, basaltic activity succeeded the rhyolites and was associated with the marine transgression. In this case the basalt accumulations were subaerial, resulting in the Patagonian plateau basalts, but once again the largest volume of basaltic volcanism coincided with the areas of greatest basin subsidence. The volcanic-arc–back-arc situation apparently continues to the present day with evidence of 'back-arc' basaltic activity in the form of the younger

PHILOSOPHICAL TRANSACTIONS OF THE ROYAL SOCIETY A MATHEMATICAL, PHYSICAL & ENGINEERING SCIENCES

activity on the Patagonian plateau. The evidence for recent activity in the calc-alkaline arc in the area described here is not so good and rests mainly with young (Miocene) ages from the batholith, as calc-alkaline volcanics of this age appear to be absent.

The general environment at least from the Upper Jurassic and possibly from the Upper Palaeozoic to the present day, has been a volcanic–batholithic arc with a back-arc basin to the east. There has usually been a continental arc backed by a continental mildly extensional, volcano tectonic rift zone, but in the Lower Cretaceous and Lower Tertiary there was an island arc with a marine back-arc basin.

Within this setting igneous petrogenesis along the arc has been related fundamentally to easterly subduction of Pacific ocean floor, with a combination of processes producing cogenetic batholithic and calc-alkaline volcanic suites. Behind the arc, igneous activity has probably been related mainly to mantle diapirism (Oxburgh & Parmentier 1977) resulting in basalts and rhyolites, the latter occurring earlier through crustal melting ahead of the rising diapir. Rhyolites are also produced in the arc zone and have probably originated through crustal melting though some may have been derived by fractionation of more basic calc-alkaline parents.

The activity within the two belts may not necessarily have been synchronous. Indeed, there is a suggestion that igneous activity in this area may be releated to two major cycles. Activity in the Middle Jurassic was predominantly in the arc but towards the end of the Jurassic there was voluminous rhyolitic volcanism behind the arc leading eventually to the opening of a marine back-arc basin, and associated basaltic volcanism in the Lower Cretaceous. Cordilleran calc-alkaline igneous activity was again important in the Middle Cretaceous (Divisadero Formation) but towards the end of Divisadero times activity apparently became less in the west where the batholith was exposed to erosion, but greater in the east where the volcanism was predominantly rhyolite. The 'back-arc' rhyolitic volcanism ended with another, more limited, marine incursion and the initiation of the basaltic volcanism of the Patagonian plateau.

Throughout this period the amount of tectonism was limited and there is very little evidence for strong horizontal movement. Thus no penetrative tectonic fabrics have been developed and no ophiolite obduction has occurred. Vertical movement has prevailed, with normal faulting particularly important in the back-arc situation. Thus the Lower Cretaceous back-arc basin may have originated largely through normal fault-controlled subsidence, and its elimination may have occurred through uplift. The minor folding seen in the area may represent cover response to vertical movement in the basement.

It may be possible to relate the geological history outlined above to major events in the spreading history of the Atlantic and Pacific oceans. In particular the period 125 to 110 Ma, identified as a period of relatively slow spreading in the Pacific by Larson & Pitman (1972), may correspond to the opening of the marine back-arc basin (Coyhaique Formation) and the limited Cordilleran igneous activity in the Lower Cretaceous. Certainly, slow spreading is more likely to allow the development of subcontinental lithothermal systems to a degree where back-arc or intraplate continental volcanoes may occur (see, for example, Gass *et al.* 1978, p. 595). Again, the high spreading rates for all the world's oceans in the period 110–85 Ma coincide with the extensive Divisadero volcanism on the arc proper which might be controlled by an increase in subduction rate consequent upon increased spreading velocities.

In a recent paper, Molnar & Atwater (1978) have suggested that old dense oceanic lithosphere will tend to sink whereas the subduction of young light oceanic lithosphere may require

an additional force. Cordilleran tectonics may be associated with 'forced' subduction of young ocean floor whereas ready sinking of old lithosphere may lead to seaward extension of the subduction site (trench) and consequent inter-arc (back-arc) spreading. This hypothesis may possibly be extended to account for the cycles of cordilleran and back-arc igneous activity defined above for the southern Andes. All the ocean floor arriving at the western margin of South America is comparatively young, but periods of high spreading, associated with relatively high heat flow, will produce thinner lithosphere and will also result in younger lithosphere arriving at the subduction zone owing to the reduced travel time from the ridge. Cordilleran tectonics and igneous activity may thus be associated with high spreading rates. Slow spreading, on the other hand, will result in the arrival of thicker, older lithosphere, and consequent seaward migration of the trench and formation of a marginal basin. Within this tectonic framework intermediate calc-alkaline igneous activity may be favoured during the high-spreading–cordilleran phases and bimodal basaltic–rhyolitic activity may characterize the slow-ocean-spreading–marginal-basin phases (Eichelberger 1978).

Finally, the area under discussion may be compared with other areas in the southern Andes and Antarctica. The general situation of a calc-alkaline volcanic–batholithic arc on the Pacific side and a volcano–tectonic depression with bimodal rhyolite–basalt volcanism behind the arc to the east is common to most of South and North America and Antarctica. If, however, detailed regional accounts are considered it is clear that significant differences exist between adjacent areas. Thus, if one compares the area considered here with the area to the south (Dalziel *et al.* 1974), the Jurassic–Lower Cretaceous histories are broadly similar with mid-Jurassic calc-alkaline volcanics rooted by the Patagonian batholith in the west, and mainly rhyolitic volcanism in the east. This stage was succeeded by the development of an island-arc along a sliver of continental crust separated from the mainland by a marine back-arc basin. Here, however, the similarities end. In the south the back-arc basin was wider and deeper with greater igneous activity and spreading, and subsequent closure of the basin resulted in ophiolite emplacement and development of strong penetrative tectonic fabrics. Volcanic activity in this area apparently stopped in the Lower Cretaceous. On the other hand, in the area described here the back-arc basin was of much more limited extent and its closure, which may have been more by vertical uplift than by horizontal movement, produced no ophiolite emplacement or penetrative fabric development. In this area the closure of the basin was followed by a period of intense Middle Cretaceous–Lower Tertiary volcanism. Oddly perhaps, the post-Jurassic history of the area considered here more closely resembles that of South Georgia (Tanner & Rex 1979) over 3000 km away, where calc-alkaline volcanics of Middle to Upper Cretaceous age (Annenkov Island Formation) occur.

It appears, therefore, that although a similar general tectonic framework of arc and back-arc has existed throughout the Andes and much of Antarctica since the Middle Jurassic there are considerable differences in the detailed geological histories of individual areas. These differences may imply that the area has developed as a series of discrete, probably fault-bounded, blocks within each of which tectonic and petrogenetic processes vary. This segmentation probably continues to the present day. The absence of recent calc-alkaline volcanism in the area studied here contrasts with its presence in the areas to the north and south. Earthquake activity is abundant north of the intersection of the Chile Rise with the continent (46 °S) and virtually absent to the south. A further implication of this is that the boundary between the fault-bounded blocks may not have shifted much through time since the boundary between the Upper

PHILOSOPHICAL TRANSACTIONS OF THE ROYAL SOCIETY A MATHEMATICAL, PHYSICAL & ENGINEERING SCIENCES

Mesozoic geological provinces probably lies between 47 °S and 51 °S, which is the northern limit of ophiolite exposure (Dalziel *et al.* 1975).

The fundamental cause of the different activity in different blocks both at present and back through geological time may be related to differences in the subduction process which may in turn be related to differences in ocean-spreading rates. Differences in the angle of subduction or in the rate of subduction could cause differences in igneous activity to develop in the different blocks. For example, low subduction angles and low subduction rates may tend to inhibit calc-alkaline igneous activity. Whatever the cause of variation between the blocks it appears that calc-alkaline activity and back-arc rhyolite–basalt activity tend not to occur at the same time within individual blocks and in this respect it may be significant that the most recent plateau basalt activity (for example on Meseta del Lago Buenos Aires) occurs at a latitude where there has been no recent calc-alkaline activity.

Conclusions

1. Igneous activity in the area described has been long lived, lasting at least from the Middle Jurassic to the present day. Throughout this period the magmatic history has been controlled fundamentally by easterly subduction at the western margin of South America.
2. Essential components in the igneous history are a calc-alkaline arc in the west and a back-arc basin in the east within which the activity has been bimodal rhyolitic–basaltic.
3. Two major cycles seem to have occurred, each beginning with calc-alkaline activity in the arc and ending with basaltic activity, immediately preceded by rhyolite volcanism in the back-arc basin.
4. The geological evolution of the area shows broad similarities with that of other areas in the Andes and Antarctica. There are, however, some significant differences which may be ascribed to different development in separate fault-bounded blocks.
5. Within the Andean–Antarctic province as a whole and within individual blocks cordilleran (calc-alkaline) and back-arc (rhyolite–basalt) igneous activity generally occurred, and still occur, at different times. The cordilleran activity appears to be favoured by more rapid ocean-floor spreading and subduction rates, and back-arc activity by slow spreading and subduction.

II. The plateau basalts

Distribution and general character of the basalts

The Patagonian basalts form part of a more extensive basaltic province that lies east of the Andes and reaches southwards from approximately the latitude of Buenos Aires (34 °S) almost to the Straits of Magellan (figure 1). Patagonia itself is defined as that part of the Argentine lying between the Rio Colorado (*ca.* 39 °S) and Tierra del Fuego. It is a vast, deeply dissected plateau, which slopes gently towards the Atlantic from the foothills of the Andes.

The older rocks of the Patagonian shield are largely obscured by Mesozoic and Tertiary rocks and it is the Jurassic–Cretaceous volcanics, volcaniclastics and associated sediments that usually form the basement to the basalt pile. The basaltic succession is often immediately underlain by a prominent tuffaceous or ignimbritic horizon, for example at Morro Negro and Chile Chico. Much of the surface of the Patagonian plateau is covered by Quaternary glacial and fluvio-glacial deposits.

This particular study is concerned with remnants of the Patagonian basalt plateau lying between about 45 and 47 °S. The locations of the principal outcrops examined, together with sample numbers, are shown on figure 6.

In this area the basalts do not extend right across to the Atlantic coast but disappear at about 68.5 °W in the vicinity of Lago Colhue Huapi. It is unlikely that they were ever continuous across the entire region and at present they constitute only about 10 % of the area studied.

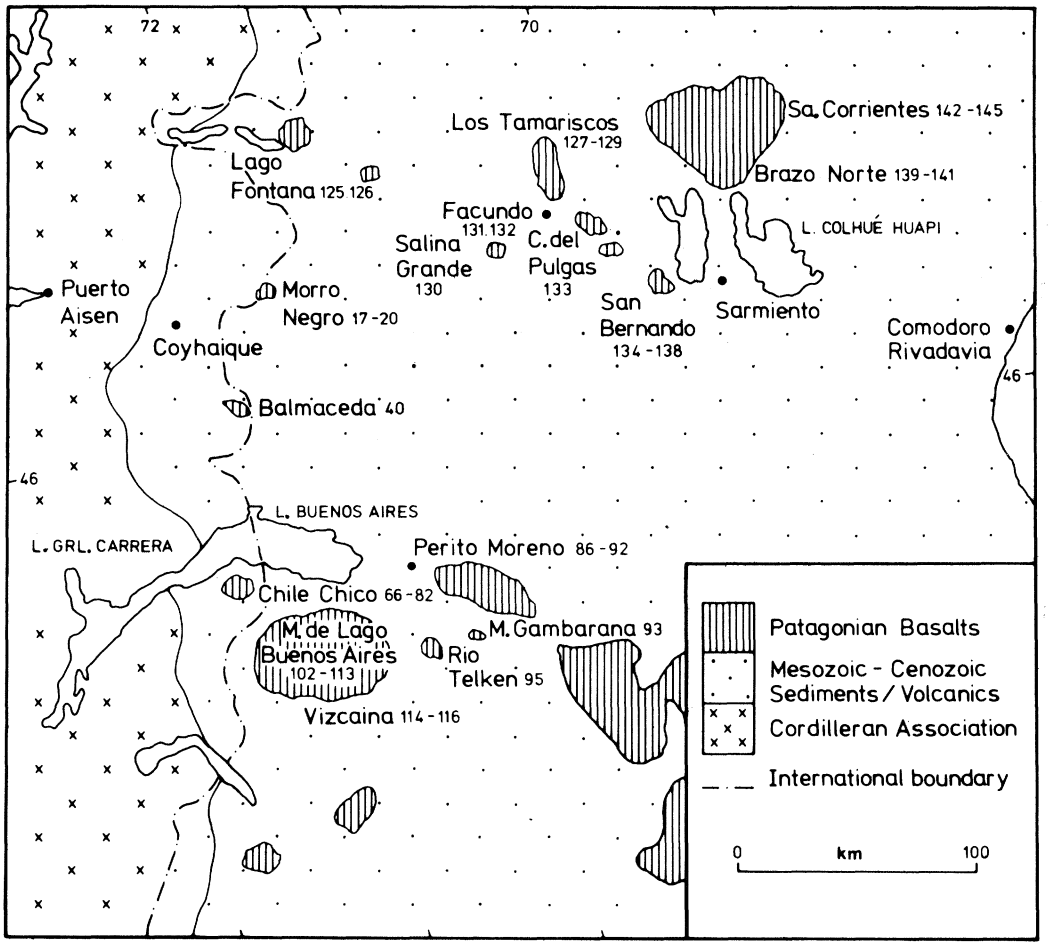

FIGURE 6. Location map of Patagonian plateau basalt outcrops around 46 °S. Sample numbers are also shown.

Though by no means confined to the more elevated tablelands, the basalts are best exposed in conspicuous isolated meseta. Here they occur as typical trap formations, rising step-like above the lower-lying Mesozoic volcanics and sediments (figure 7, plate 1). They reach their maximum development in the Meseta del Lago Buenos Aires which is situated immediately south of the lake of that name close to the border with Chile at *ca.* 46.5 °S: the region is about 60 km across and reaches approximately 2000 m above sea-level. The total thickness of the basalt pile in the Meseta del Lago Buenos Aires is about 700 m, though if the post-plateau cones and associated surface flows were included the thickness would locally be nearer 1 km.

Smaller meseta occur at Morro Negro, Morro Gambarana and in the Sarmiento region

around Lago Musters. Alkaline intrusive complexes of Tertiary age from the Sarmiento area have been described by Villar & Pezzutti (1976).

Numerous outcrops also occur westwards from here to Facundo and in the region of Lago Fontana near the frontier with Chile. Several basalt outcrops occur in the foothills of the Andes on the Chilean side of the border, the main one of which is at Chile Chico immediately south of Lago General Carrera (Lago Buenos Aires). The basalts are here reduced to about 300 m

TABLE 3. POTASSIUM–ARGON AGE DETERMINATIONS

(Abbreviations; bio, biotite; w.r., whole rock; ^{40}Ar rad, ^{40}Ar radiogenic.)

sample no.	material analysed	K(%)	volume ^{40}Ar rad 10^{-5}cm^3/g^{-1}	^{40} Ar rad (%)	age/Ma
P12	bio	7.27	2.8253	90.5	97 ± 4
P19	w.r.	0.679	0.2087	74.4	77 ± 3
P40	w.r.	0.994	0.1787	66.6	46 ± 2
P64	w.r.	0.858	0.01233	11.8	3.7 ± 0.2
P66	w.r.	0.529	0.08869	66.1	43 ± 2
P67	w.r.	0.878	0.1430	71.3	42 ± 2
			0.1454	22.2	
	w.r.	0.917	0.1544	43.4	43 ± 2
P68	w.r.	0.730	0.1498	28.2	52 ± 2
			0.1480	67.9	
	w.r.	0.761	0.1561	57.6	52 ± 2
P70	w.r.	0.481	0.1073	57.2	57 ± 3
P71	w.r.	0.927	0.1988	74.8	54 ± 2
P72	w.r.	1.07	0.1919	74.0	46 ± 2
P93	w.r.	0.954	0.03815	47.9	10 ± 0.4
P111	w.r.	0.590	0.02301	18.5	10 ± 0.5
P114	w.r.	1.74	0.00945	11.3	1.4 ± 0.1
P115	w.r.	1.72	0.00567	6.6	0.8 ± 0.1
P117	w.r.	1.21	0.3869	80.5	81 ± 3
P120	w.r.	1.29	0.3995	77.4	78 ± 3
P124	w.r.	1.26	0.3875	83.9	78 ± 3
P126	w.r.	2.58	0.03615	23.0	3.6 ± 0.2
P129	w.r.	1.19	0.01498	10.3	3.2 ± 0.2
P130	w.r.	1.62	0.01631	13.3	2.6 ± 0.2
P131	w.r.	1.44	0.1217	59.8	22 ± 1
P132	w.r.	1.33	0.1096	50.0	21 ± 1
P133	w.r.	1.55	0.01658	23.4	2.7 ± 0.2
P135	w.r.	1.15	0.1072	43.1	24 ± 1
P139	w.r.	1.60	0.01765	30.3	2.8 ± 0.2

Decay constants used were as recommended in Steiger & Jager (1977).
The K analysis was made by A. R. Gledhill.
All samples are lavas apart from P12 which is a grey granite from 12 km east of Puerto Aisen.

thick and rest on Mesozoic tuffs and ignimbrites. The lava pile is cut by volcanic necks or plugs which may once have formed feeders to the surface cones and flows: one of these at Cerro Lapiz (figure 8, plate 1) contains abundant small ultramafic xenoliths. The Chile Chico meseta reaches a maximum height of 2190 m at Cerro Pico Sur. Individual flows range in thickness from 5 m to about 25 m and are occasionally separated by intrabasaltic detrital or tuffaceous horizons.

AGE RELATIONS IN THE BASALT SUCCESSION

Potassium–argon ages have been determined at the Department of Earth Sciences, Leeds University on 24 lavas from this part of Patagonia (see table 3). Analytical procedures are as

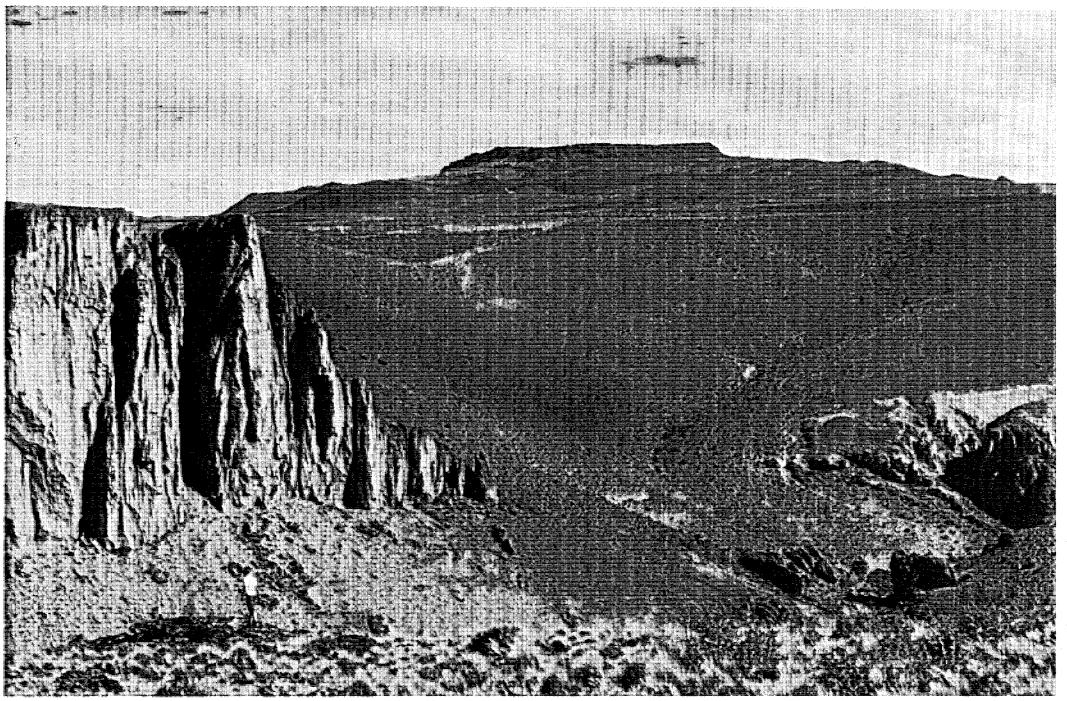

FIGURE 7. Small basalt meseta showing trap features overlying Mesozoic ignimbrite (cliffs in foreground); Cueva de los Manos 47° 10′S, 70° 28′W.

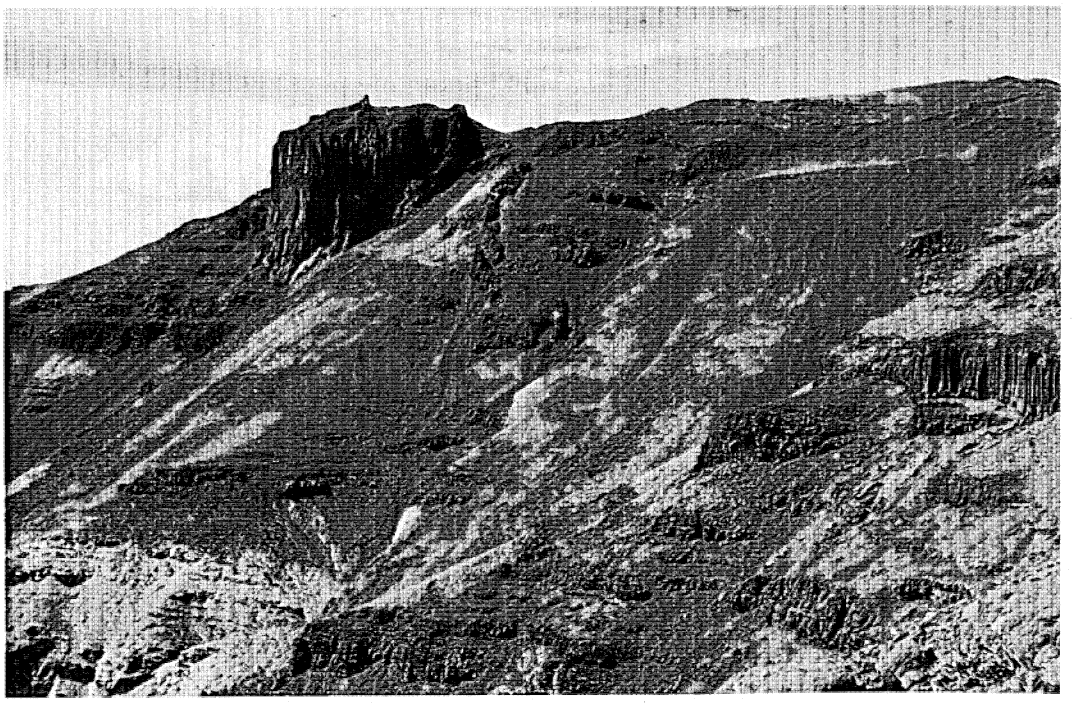

FIGURE 8. Patagonian basalts at Chile Chico, cut by the Cerro Lapiz plug, a locality for ultramafic xenoliths.

(*Facing p.* 126)

PHILOSOPHICAL TRANSACTIONS OF THE ROYAL SOCIETY A MATHEMATICAL, PHYSICAL & ENGINEERING SCIENCES

FIGURE 10. Cerro Colorado and other post-plateau cones on surface of Meseta del Lago Buenos Aires; basanite flow in foreground.

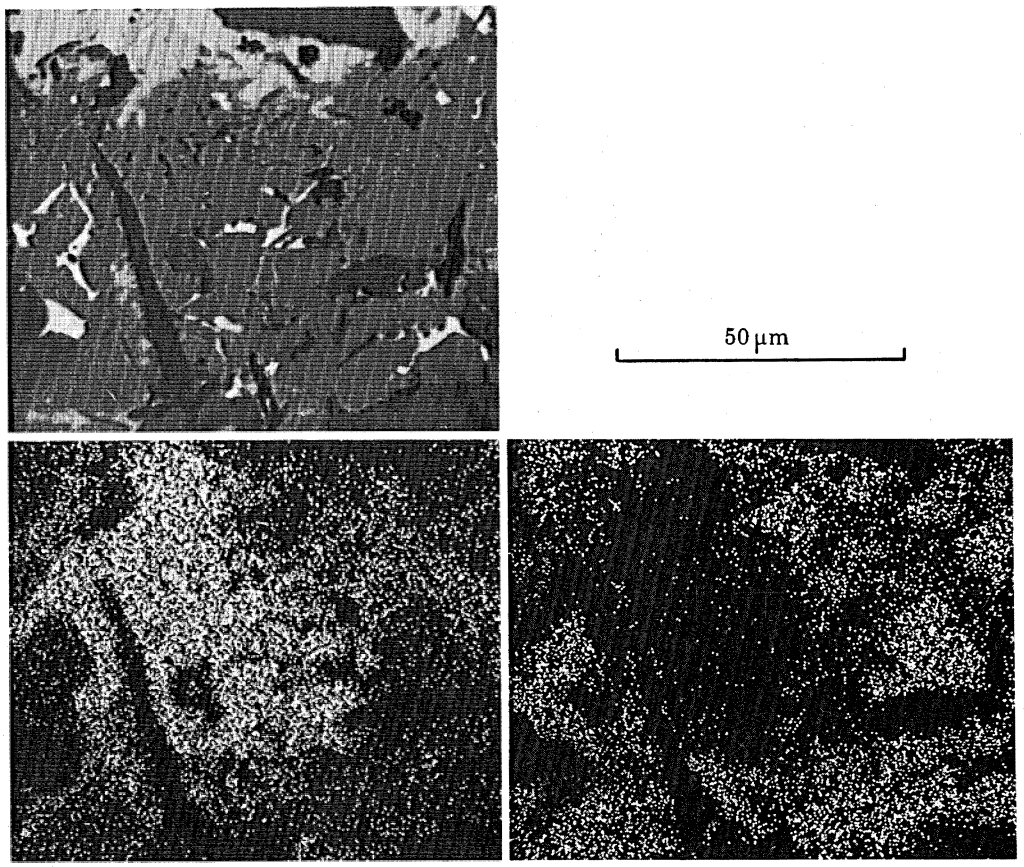

FIGURE 11. Electron microprobe images illustrating occurrence of leucite (high K and low Na concentrations) in basanite P90: top, back-scattered electron image; bottom left, K distribution; bottom right, Na distribution.

PHILOSOPHICAL TRANSACTIONS OF THE ROYAL SOCIETY A MATHEMATICAL, PHYSICAL & ENGINEERING SCIENCES

TABLE 4. PALAEOMAGNETIC AND ASSOCIATED K–Ar AGE DETERMINATIONS

sample no. PEB	sample no. RC	locality	palaeomagnetism (polarity)	K–Ar age/Ma
		Meseta Del Lago Buenos Aires area		
P87	3	basalt from side of Rio Deseado Valley	—	3.4 ± 0.4
P88	5	post-glacial basalt from Cerro Volcan	normal	0.3 ± 0.1
P90	7	leucite basanite, Arroyo Page 17 km ESE of Perito Moreno	normal (similar to P88)	0.2 ± 0.1
P92	9	basalt forming upper part valley side, Arroyo Page, as above	reversed	20 ± 2
P94	10*a*	flow capping Meseta Gambarana	oblique/normal	—
	10*b*		normal	
	10*c*		normal	
P95	11*a*	young basanite, ruta 40; 6 km S of Rio Telken	normal	—
	11*b*			
	11*c*			
P102	12	flow from young cone on Meseta Lago Buenos Aires, N of Cerro Colorado	reversed	1.8 ± 0.5
P103	13	young basaltic flow E of Cerro Colorado		1.8 ± 0.5
P104	14	young flow 1 km S of Puesto El Perdido	reversed	
P109	15	lower part of top flow in crater wall Laguna Honda	—	1.6 ± 0.5
P110	16*a*	edge of Meseta, S of Cerro Puntudo	*a*, *c* oblique/normal	9.0 ± 1
	16*b*		*b* normal	
	16*c*			
P111	17*a*	southern edge of Meseta above Ea Vizcaina	*a* normal	10 ± 1
	17*b*		*b* reversed	
P114	18*a*	basalt in Arroyo Eike SE of Meseta Del Lago	*a* reversed	—
	18*b*	Buenos Aires	*b* oblique/reversed	—
P116	19*a*	lower flow, locality as above	oblique/reversed	—
P115	20	as above, but topographically lower (fourth level)	normal	—
P91	8	rhyolitic ignimbrite beneath basalts in Arroyo Page	—	155 ± 15
		Lago Fontana area		
P122	23	Ea El Triunfo 14 km W of Alto Rio Senguerr	normal	—
P125	24	north side of Lago Fontana	normal	—
P126	25	as above, Arroyo Rio Gato	normal	—
		Facundo area		
P127	26	13 km SE of Los Tamariscos		20 ± 2
P130	27	Cerro El Pedrero, 3 km S of volcanic cone, above Salina Grande	normal	—
P133	29	small meseta Ruta 20, 23 km SE of Facundo	normal	—
		Sarmiento area		
P137	30*a*	Cerro San Bernardo	normal	—
	30*b*		normal	
	30*c*		oblique/normal	
P140	31	N of Sarmiento, edge of meseta N of Lago Colhue Huapi	—	$3.0 \pm 5{\cdot}0$
P142	32*a*	N of Sarmiento, edge of meseta	*a* oblique/normal	—
	32*b*	N of Lago Colhue Huapi	*b* variable?	—
P143	33	NE of Ea Molle Grande	—	25 ± 2

described in Briden *et al.* (1979). Additional K–Ar ages were determined in Buenos Aires in conjunction with palaeomagnetic measurements. The polarity and ages of these samples are given in table 4.

The radiometric dating indicates that an extraordinarily protracted period of volcanism is represented in the Patagonian succession, which apart from a break of about 20 Ma (which could be a reflexion of inadequate sampling) ranges from Upper Cretaceous to nearly historic. The time span represented is therefore considerably longer than that determined for other major plateau basalt sequences such as the Columbia River basalts (17–6 Ma, Swanson & Wright (1979) the Karroo province (190–154 Ma, Cox (1972)) or the Deccan plateau (65–37 Ma, Ghose 1976).

The oldest basalts encountered occur some 15 km east of Alto Rio Senguerr on Estancia El Triunfo. These samples are not ideal for dating since there is some alteration and they contain a few zeolites: however K–Ar dating on three separate flows indicated ages in the range 78–81 Ma. Some 60 km southwest of here straddling the frontier with Chile near Coyhaique Alto is the small meseta of Morro Negro where a fresher lava flow from close to the base of the pile has yielded a K–Ar age of 77 Ma. One of the most complete successions through the basalt pile is to be found in the cliffs below Cerro Lapiz in the Chile Chico area. An unexpected substantial break is represented in the sequence. The oldest flows are in the range 43–56 Ma and the highest of this group (P66) is immediately overlain by a brown tuffaceous or volcaniclastic horizon. The lava that rests on top of this bed is the youngest flow extensively developed across the surface of the plateau, dates at only 3.7 Ma (figure 9). In the same section below Cerro Lapiz Charrier *et al.* (1979) also report two units with ages of at least 57 Ma for the older and of 16–4.4 Ma for the younger.

Elsewhere in the region studied the lowermost flows in the plateau date at between 20–25 Ma. The lava forming the main surface of the plateau, particularly in the Meseta del Lago Buenos Aires and Meseta Gambarana has an age of about 9 Ma.

The evidence therefore suggests that within the main part of the plateau there may be two cycles of activity, an older one commencing at Senguerr and affecting Morro Negro at approximately the same time but reaching Chile Chico, further south and west, some 20 Ma later. There is no indication of any activity in the region between 43 Ma and 25 Ma. The second cycle appears to have started further to the east in the Sierra Corrientes north of Lago Coluhue Huapi about 25 Ma ago, and the onset of volcanism occurred at successively later times towards the west. There are insufficient ages to be sure whether volcanism was episodic or almost continuous throughout this second cycle but it is apparent that activity ceased approximately 9 Ma ago with the last extensive flows which now form the top unit of the plateau.

Younger, post-plateau flows and pyroclastics are best developed on the surface of the Meseta del Lago Buenos Aires (figure 10, plate 2) and the summit of Chile Chico. All of the flows dated from this group are younger than 4 Ma suggesting that there was a gap of about 5 Ma between the cessation of fissural activity on the plateau and the onset of these late small central eruptions. Ages obtained on the post-plateau volcanics suggest that minor activity was nearly continuous from about 3.7 Ma almost to the present day. The youngest K–Ar age obtained (0.2 Ma) was on a lava from the Perito Moreno area where the well preserved morphology of cinder cones and lava surfaces points to very recent activity, though no historic eruptions have been recorded.

The present relief of the plateau surface is largely determined by the scarcely modified thinly spread products of the late volcanism: no substantial strato-volcanoes have been built on the

PHILOSOPHICAL TRANSACTIONS OF THE ROYAL SOCIETY A MATHEMATICAL, PHYSICAL & ENGINEERING SCIENCES

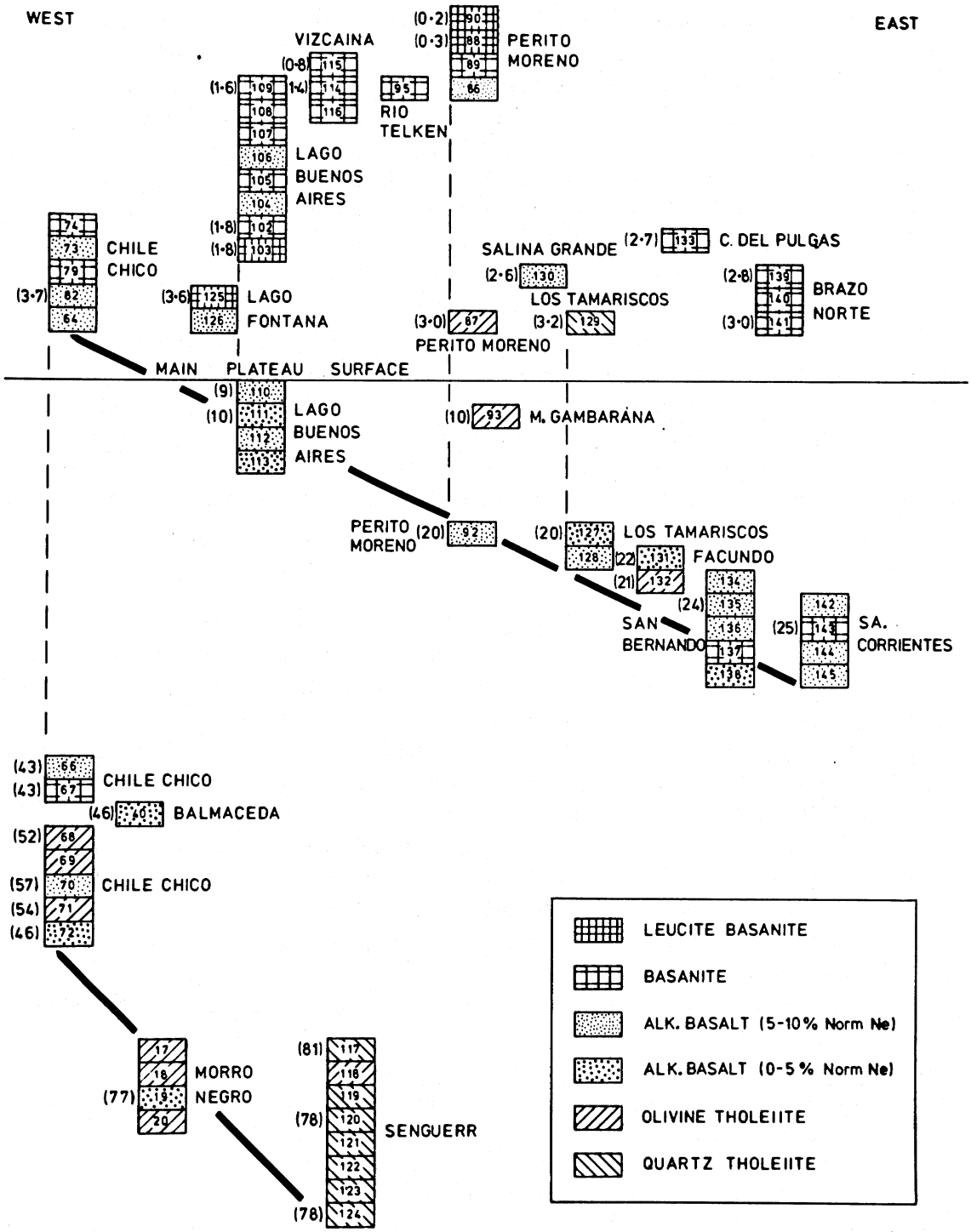

FIGURE 9. Stratigraphic relations in the Patagonian basalts arranged in approximate geographical order from west to east across Aisen, Chubut and Santa Cruz. Shading indicates compositions; sample numbers are given within rectangles. Radiometric ages in Ma are shown in parentheses at the left-hand side of sections.

PHILOSOPHICAL TRANSACTIONS OF THE ROYAL SOCIETY A MATHEMATICAL, PHYSICAL & ENGINEERING SCIENCES

plateau. The young post-glacial cones and flows are usually quite distinct from the main plateau volcanics which are often covered by glacial debris. Some of the young lavas have been channelled down valleys cut into the edges of the plateau and have travelled as confined valley flows some distance from the meseta. Sometimes, as along the southern edge of Meseta del Lago Buenos Aires near Estancia Vizcaina, lavas have spilled over the edge of the plateau and spread out at the foot of the meseta. They have produced a series of low-lying lava terraces which sometimes give the misleading impression of being outliers of the lower part of the main plateau sequence.

The entire range of ages reported for the Patagonian basalts from 41 to 52 °S (Ramos *et al.* 1980) are represented in the area studied here. The maximum ages of *ca.* 80 Ma all occur in the northwestern part of Patagonia between latitudes 41 and 46 °S. At the other extreme only relatively young lavas (1.24–0.17 Ma) have been reported from the Pali-Aike volcanic field in the far south-east of Patagonia (Skewes & Stern 1979).

In their review of the magmatic evolution of the Austral Patagonian Andes, Ramos *et al.* (1980) distinguish four different cycles of activity. Although their Upper Cretaceous and Lower Tertiary groups are readily recognizable as the Senguerr–Morro Negro and Chile-Chico–Balmaceda sections described here, there is less correspondence in the younger groupings. The absence of basalts in the age range 77–57 Ma is sustained but the apparent break between *ca.* 43 and 25 Ma suggested by the results presented here (figure 9) does not appear to apply over the entire region (Ramos *et al.* 1980, figure 11).

Petrography and compositional variations

The Patagonian lavas appear fairly uniform in the field with most being dark grey aphyric or sparsely porphyritic rocks. Some of the flows, especially near the top of the plateau are plagioclase–phyric, and olivine–pyroxene–phyric lavas occur in the post-plateau series. However, the compositional variations proved on chemical analysis to be much greater than had been suspected in the field. The lavas range from quartz tholeiites through olivine tholeiites to alkali basalts, basanites and ultimately to highly potassic leucite basanites. The following generalizations can be made about the distribution of different rock types within the succession.

(i) Quartz tholeiites and olivine tholeiites are concentrated in but not confined to the older part of the plateau. Occasionally tholeiitic lavas are to be found in the upper part of the plateau (for example P93 from Meseta Gambarana) and also as post-plateau flows, (for example P129 from 24 km south of Los Tamariscos).

(ii) Alkali basalts are concentrated in the late plateau group but are also represented in both the older and post-plateau series.

(iii) The post-plateau flows are predominantly basanites.

(iv) Leucite basanites, though not especially common, are entirely confined to the post-plateau group (figure 11, plate 2).

An idealized, diagrammatic cross section showing the plateau and post-plateau age and compositional relations is illustrated in figure 12.

More detailed geographical, stratigraphic and compositional relations, illustrating the distribution of K–Ar ages and principal grouping of the basalts are shown in figure 9.

The progressive modal shift of the rock types from tholeiites in the early plateau to alkali basalts in the late plateau and basanites in the post-plateau lavas is illustrated by histograms in figure 13. However, since these plots are based on the collected and analysed samples, the peaks

are likely to be exaggerated through over-collecting of the post-plateau samples. Although they should not be regarded as volumetrically representative of the proportions in the sequence, the general modal migration is considered a real one. The overall proportions of rock types in the succession are illustrated in figure 14 which suggests that alkali basalts are dominant. Again, the basanites have probably been over-emphasised, and a diagram based on volume relations would probably show a more distinct mode in the alkali basalt range.

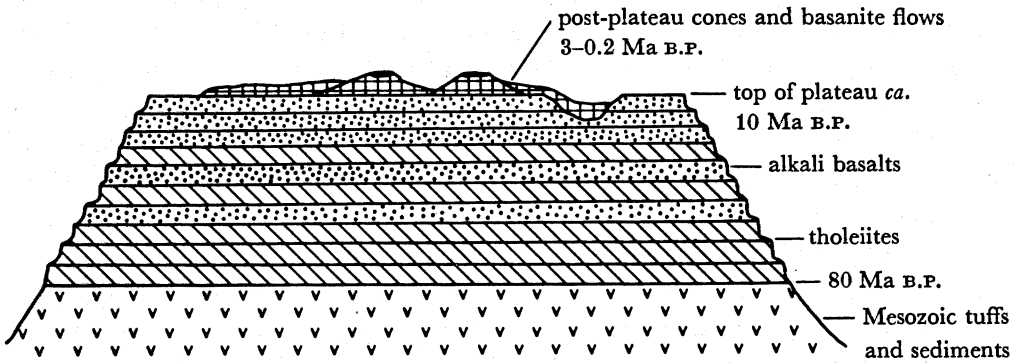

FIGURE 12. Diagrammatic cross section through Patagonian plateau illustrating generalized sequence of rock types and relative ages.

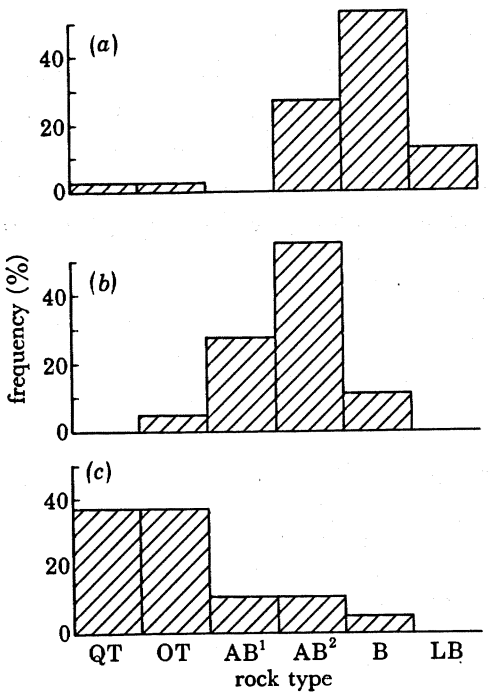

FIGURE 13. Frequency distribution of rock types at different stratigraphic levels in the Patagonian plateau (based only on samples in collection): (*a*) post-plateau; (*b*) late-plateau; (*c*) early plateau. QT, quartz tholeiite, OT, olivine tholeiite, AB^1, alkali basalt (less than 5 % normative nepheline), AB^2, alkali basalt (5–10 % normative nepheline), B, basanite, LB, leucite basanite.

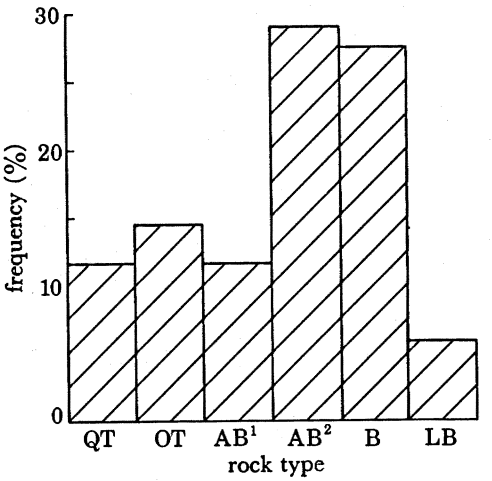

FIGURE 14. Overall frequency distribution of rock types in the Patagonian plateau (based only on rock types in collection). Rock-type abbreviations are given in figure 13.

Typically the *quartz tholeiites* (e.g. P120) are almost aphyric lavas with small sparsely distributed olivine phenocrysts in a matrix of plagioclase laths and granular pyroxenes. The *olivine tholeiites* tend to be coarser grained with olivine and sometimes plagioclase phenocrysts in a mesostasis dominated by clinopyroxene. A distinctive feature of the olivine tholeiites is the rather patchy occurrence of an ophitic to subophitic texture (for example P69). *Alkali basalts* are characterized by fairly abundant olivine phenocrysts, often partially altered to iddingsite, and by a pale pink–brown zoned titaniferous clinopyroxene. The matrix is variable from a very fine grained pilotaxitic texture (for example P64) to a rather coarse subophitic texture seen in some of the flows near the top of the plateau (for example P111 from Meseta del Lago Buenos Aires).

The *basanites* are characterized by an even greater abundance of olivine phenocrysts, sometimes accompanied by clinopyroxene, though plagioclase is usually the second phase to crystallize, and the strongly coloured pyroxene tends to be restricted to fairly large grains in the matrix. In the *leucite basanites* clinopyroxene becomes a more conspicuous phenocryst phase: although olivine remains dominant, plagioclase is greatly reduced in abundance. Apart from the phenocryst minerals the distinctive feature of the leucite basanites is the quench-like appearance of the ground-mass. There is a complete lack of any preferred orientation so that sparsely distributed and randomly arranged feldspar laths and pyroxene clusters are set in a fine matrix of pyroxene and spiky ilmenites, associated with patches of nepheline, sanidine and leucite.

Mineralogy

Examples of mineral compositions are given in table 5.

Most minerals are quite strongly zoned except for those in the ultra-basic nodules (peridotite and spinel lherzolite) from the basaltic neck at Cerro Lapiz. Olivine and pyroxene crystals reach their most magnesian compositions in these nodules, approaching forsterite, enstatite and diopside. Compositions of phases in the ultramafic nodules are similar to those reported by Skewes & Stern (1979) from Palei-Aike except that garnet and phlogopite-bearing types do not feature in the Cerro Lapiz suite.

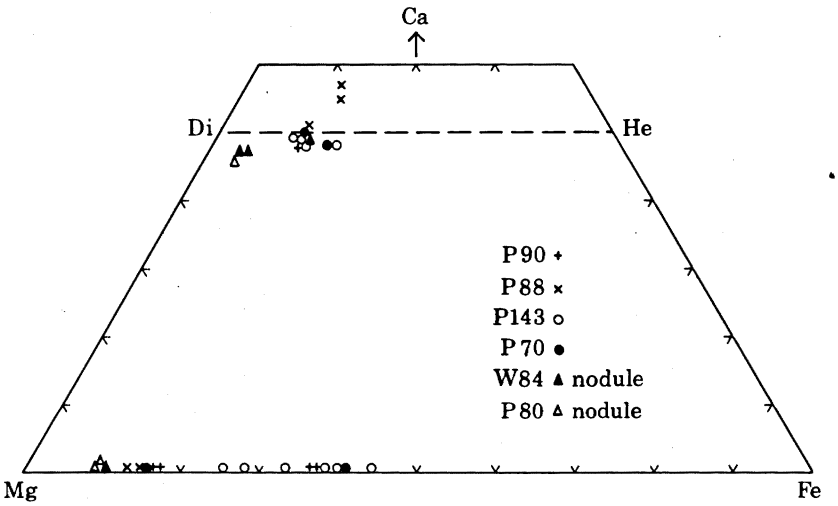

Figure 15. Plot of Ca–Mg–Fe ratios in analysed clinopyroxenes and Mg–Fe ratios in olivines from Patagonian lavas and associated ultramafic nodules.

Olivine phenocrysts in the lavas reach Fo_{87}, and smaller crystals are zoned down to Fo_{56}. Magnesium/iron ratios of the olivines and Ca/Mg/Fe ratios of the pyroxenes are plotted in figure 15. Most clinopyroxenes in the lavas cluster about a magnesian salite composition, bordering on the diopside field. In the alkali basalt (P70) and in the basanite (P143) there is evidence that individual crystals are zoned outwards to slightly more Fe-rich but lower Ca compositions. They are following a similar trend to that well established for relatively Ca-rich clinopyroxenes in alkali–basalt magmas (Wilkinson 1956). However, in the leucite basanite (P88) the trend from core to rim is towards high calcium aluminous titanaugite (table 5, no. 5) with progressively lower silica content. The trend exhibited by clinopyroxenes in these highly undersaturated Patagonian lavas is similar to that which has been described in basanite lavas by Kushiro (1960) and Le Bas (1962).

Plagioclase phenocrysts are normally zoned within the bytownite–labradorite–andesine range but ground-mass feldspars are extremely varied in composition and include sandine, anorthoclase and almost pure albite. Small patches of leucite have been positively identified in the ground-mass of the leucite basanites (figure 11), and an analysis of a leucite grain is shown in table 6 (no. 6). This analysis is very similar to that of leucite from a leucitite lava of Mount Mikeno, Lake Kivu (Sahama 1952). However, in the Patagonian lavas leucite never occurs as phenocrysts and is confined to slightly brownish patches or aggregates in the matrix where it is usually associated with clearer areas of nepheline. The leucite is not readily identifiable by

TABLE 5. MINERAL COMPOSITIONS

(Abbreviations: cpx., clinopyroxene; fsp.phen., feldspar phenocrysts; ol.phen., olivine phenocrysts opx., orthopyroxene)

P90 leucite basanite
ol. phen.: Fo_{84}, Fo_{83}
small olivines: Fo_{64}, Fo_{63}
cpx: $Ca_{48}Mg_{40}Fe_{12}$
fsp. phen.: $Or_3Ab_{38}An_{69}$, $Or_4Ab_{27}An_{69}$
+ nepheline and leucite in ground-mass

P88 leucite basanite
ol. phen.: Fo_{87} zoned to rim Fo_{85}
cpx.: $Ca_{51}Mg_{38}Fe_{11}$ zoned to rim $Ca_{57}Mg_{31}Fe_{12}$
$Ca_{55}Mg_{32}Fe_{13}$
fsp: $Or_3Ab_{25}An_{72}$

P143 basanite
olivines: Fo_{75-62}, Fo_{72-60}, Fo_{67-56}
cpx.: $Ca_{49}Mg_{40}Fe_{11}$ zoned to rim $Ca_{48}Mg_{36}Fe_{16}$
$Ca_{48}Mg_{40}Fe_{12}$ zoned to rim $Ca_{48}Mg_{31}Fe_{15}$
$Ca_{49}Mg_{41}Fe_{10}$

P70 alkali basalt
olivine: Fo_{85} zoned to rim Fo_{59}
cpx.: $Ca_{50}Mg_{39}Fe_{11}$ zoned to rim $Ca_{48}Mg_{37}Fe_{15}$
fsp.: $Or_{22}Ab_{33}An_{45}$, $Or_4Ab_{87}An_9$, $Or_{88}Ab_9An_3$, $Or_0Ab_{99}An_1$

P80(*a*) lherzolite nodule
olivine: Fo_{91}
cpx.: $Ca_{46}Mg_{50}Fe_4$
opx.: En_{91}

W84 peridotite nodule
olivine: Fo_{90}
large cpx.: $Ca_{47}Mg_{48}Fe_5$, $Ca_{47}Mg_{49}Fe_4$
small cpx: $Ca_{49}Mg_{39}Fe_{12}$

normal optical methods and its presence only becomes apparent during microprobe analysis. Its mode of occurrence in the Patagonian lavas resembles that in the potassic lavas of Tristan da Cunha (Le Maitre & Gass 1963).

TABLE 6. ANALYSES OF PYROXENES AND LEUCITE

(Data are given as % by mass.)

	(1)	(2)	(3)	(4)	(5)	(6)
S_iO_2	55.60	53.22	51.52	48.07	39.71	54.05
TiO_2	0.11	0.55	1.42	2.84	4.57	—
Al_2O_5	4.06	6.12	2.24	6.27	10.28	21.22
FeO	5.96	2.36	8.84	6.55	7.01	—
MnO	0.14	0.00	—	0.10	0.00	—
MgO	34.34	15.61	12.14	12.27	9.68	—
CaO	0.54	20.20	21.95	20.99	25.29	1.80
Na_2O	0.09	1.74	—	0.47	0.61	0.17
K_2O	—	—	—	—	—	21.29
total	100.84	99.80	98.11	97.56	97.15	98.53
Ca	1	46	48	48	57	
Mg	90	50	37	40	31	
Fe	9	4	15	12	12	

(1) Enstatite from lherzolite nodule P80, Cerro Lapiz.
(2) Diopside from lherzolite nodule P80, Cerro Lapiz.
(3) Rim of salite from alkali basalt P70, Chile Chico.
(4) Salite from leucite basanite P90, Arroyo Page, Perito Moreno.
(5) Titanaugite from leucite basanite P88, Perito Moreno.
(6) Leucite from matrix of leucite basanite P90, Perito Moreno.

Analyses were made with the Jeol microprobe at the Department of Earth Sciences, Leeds University.

GEOCHEMISTRY

In spite of the general shift from tholeiitic to alkalic and basanite lavas up the plateau sequence there are few systematic variations so far as major elements are concerned. For example there is no regular covariation of total alkalis with silica. The post-plateau, basanitic rocks tend to have lower silica and higher alkalis but in fact the alkali content of some of the early plateau tholeiites with relatively high silica is very similar to many of the later alkali basalts. It is possible that the lavas of this area belong to two distinct series and that opposing alkali–silica trends conceal any systematic variation. The early plateau lavas of Morro Negro, Senguerr and part of the Chile Chico succession seem to represent a calc-alkali or tholeiitic group in which total alkalis tend to increase with increasing silica, perhaps owing to low pressure fractionation effects. The later more alkalic lavas show a contrary trend of increasing alkalis linked to decreasing silica. The result is comparable alkali levels at two separate silica levels (e.g. *ca.* 46 % and 53 % SiO_2). The high alkali content of the low-silica lavas cannot be ascribed to any low pressure fractionation effect. The silica range of all but the early plateau group is comparable with that of the Palei-Aike volcanics from southern Patagonia (Skewes & Stern 1979), but the latter are less strongly undersaturated. Chemical analyses and C.I.P.W. norms of the lavas from the area studied are given in table 7.

The early tholeiitic lavas have low MgO contents (less than 6 %) whereas alkali basalt and basanites contents are consistently higher than this up to almost 11 %. Ratios of Fe/(Fe + Mg) show little systematic variation with other geochemical parameters, with rock type or with stratigraphic position. There is perhaps a slight tendency for the ratio to be higher in the early plateau lavas and also higher in the Senguerr sequence than in the Morro Negro or Chile

TABLE 7. CHEMICAL ANALYSES AND C.I.P.W. NORMS OF PATAGONIAN LAVAS

(Samples are arranged in approximate stratigraphic order, from base to top of pile. The norm was calculated on the basis of Fe_2O_3 as 15% of total iron oxides. Data are given for major elements as % by mass; for trace elements in μg/g.)

EARLY PLATEAU (pre-40 Ma)

sample no. (P) . . .	124	121	120	119	117	20
SiO_2	51.76	51.43	51.65	51.97	52.62	50.85
TiO_2	1.75	1.65	1.69	1.67	1.70	1.39
Al_2O_3	16.94	17.04	16.85	16.78	17.00	17.97
$Fe_2O_{3,\,tot}$	9.75	9.94	9.88	9.81	10.05	8.92
MnO	0.18	0.19	0.19	0.18	0.17	0.15
MgO	4.43	4.43	4.53	4.20	4.14	5.05
CaO	7.64	7.56	7.57	7.52	7.55	9.37
Na_2O	3.85	3.90	3.79	4.00	3.94	3.85
K_2O	1.51	1.54	1.54	1.46	1.47	0.67
P_2O_5	0.84	0.93	0.95	0.95	0.95	0.39
total	98.65	98.61	98.64	98.54	99.59	98.61
trace elements						
Cr	124	96	101	102	99	159
Co	20	28	26	28	23	30
Ni	48	39	35	36	31	53
Cu	45	42	57	38	45	61
Zn	94	99	100	110	101	88
Pb	9	12	14	9	9	<3
Rb	29	28	30	23	27	16
Sr	536	543	557	546	540	414
Y	42	44	45	44	45	30
Zr	330	351	384	342	349	200
Nb	17	19	20	20	18	5
Ba	568	620	572	597	626	169
C.I.P.W. norms						
Qz	0.17	0.35	0.26	1.37	2.11	—
Or	9.10	9.28	9.28	8.81	8.75	4.02
Ab	33.34	33.76	32.83	34.61	33.76	33.25
An	25.03	24.99	24.97	24.07	24.66	30.43
Lc	—	—	—	—	—	—
Ne	—	—	—	—	—	—
Di	6.68	5.86	5.85	6.36	5.73	11.76
Hy	18.12	16.96	19.08	15.95	16.12	11.12
Ol	—	—	—	—	—	2.75
Mt	2.17	3.39	2.20	3.35	3.39	3.04
Il	3.40	3.21	3.29	3.25	3.27	2.70
Ap	2.03	2.24	2.29	2.29	2.26	0.94

sample no. (P). . .	18	17	71	70	69	68
SiO_2	50.60	50.50	49.11	47.11	48.03	47.83
TiO_2	1.63	1.49	2.93	2.03	1.91	2.51
Al_2O_3	17.38	17.58	15.82	15.31	15.65	16.54
$Fe_2O_{3,\,tot}$	9.64	9.13	10.94	12.43	13.07	12.03
MnO	0.16	0.15	0.14	0.18	0.19	0.17
MgO	5.49	5.44	6.24	9.59	8.81	6.41
CaO	9.02	9.40	8.94	8.15	8.63	9.75
Na_2O	3.97	3.70	3.49	4.41	2.89	3.23
K_2O	0.77	0.59	1.33	0.62	0.51	1.00
P_2O_5	0.43	0.49	0.67	0.42	0.37	0.51
total	99.09	98.47	99.61	100.25	100.06	99.98

PHILOSOPHICAL TRANSACTIONS OF THE ROYAL SOCIETY A MATHEMATICAL, PHYSICAL & ENGINEERING SCIENCES

TABLE 7 (*cont.*)

sample no. (P) ...	18	17	71	70	69	68
			trace elements			
Cr	147	182	266	337	276	209
Co	28	33	35	44	54	38
Ni	58	65	90	130	156	61
Cu	70	54	41	76	69	65
Zn	96	91	119	89	110	92
Pb	6	7	13	3	< 3	8
Rb	16	11	18	15	7	14
Sr	429	428	626	325	294	477
Y	30	30	30	22	20	24
Zr	209	191	228	135	102	161
Nb	11	8	35	24	12	23
Ba	194	188	335	194	119	194
			C.I.P.W. norms			
Qz	—	—	—	—	—	—
Or	4.61	3.55	7.98	3.72	3.01	5.97
Ab	34.18	32.07	29.95	25.77	24.79	27.58
An	27.78	30.34	23.87	20.35	28.51	27.98
Lc	—	—	—	—	—	—
Ne	—	—	—	6.39	—	—
Di	12.07	11.55	13.55	14.32	10.00	14.36
Hy	7.84	12.24	5.18	—	12.53	0.86
Ol	6.07	4.16	9.85	21.86	13.73	14.60
Mt	3.26	2.03	2.41	2.73	2.87	2.64
Il	3.15	2.91	5.64	3.89	3.67	4.80
Ap	1.04	1.18	1.60	0.99	0.90	1.23
			LATE PLATEAU (25–9 Ma)			
sample no. (P) ...	40	67	66	144	136	132
SiO_2	45.12	44.35	43.16	45.49	45.46	50.07
TiO_2	3.04	3.11	3.72	2.28	2.46	2.40
Al_2O_3	14.90	14.98	14.66	14.86	15.03	15.22
$Fe_2O_{3,\,tot}$	11.81	12.71	14.62	12.18	12.51	11.09
MnO	0.17	0.19	0.22	0.16	0.17	0.12
MgO	8.63	9.43	8.59	9.96	9.04	8.74
CaO	9.38	10.30	10.57	8.65	8.86	8.01
Na_2O	3.43	3.86	3.15	3.52	3.84	3.45
K_2O	1.19	1.13	0.67	1.55	1.05	1.82
P_2O_5	0.79	0.90	0.90	0.48	0.63	0.57
total	98.46	100.96	100.26	99.13	99.05	101.49
			trace elements			
Cr	239	222	277	247	230	209
Co	40	41	52	45	40	43
Ni	117	104	198	142	144	127
Cu	73	48	55	68	73	31
Zn	113	93	95	94	96	106
Pb	3	5	< 3	< 3	7	< 3
Rb	22	23	13	23	19	29
Sr	713	881	257	631	715	572
Y	16	26	24	18	20	19
Zr	268	240	240	154	183	153
Nb	57	74	68	37	45	45
Ba	354	470	489	320	418	332

PHILOSOPHICAL TRANSACTIONS OF THE ROYAL SOCIETY A MATHEMATICAL, PHYSICAL & ENGINEERING SCIENCES

TABLE 7 (*cont.*)

sample no. (P) ...	40	67	66	144	136	132
			C.I.P.W. norms			
Qz	—	—	—	—	—	—
Or	7.21	6.68	4.02	9.34	6.32	10.70
Ab	20.94	13.44	16.42	17.87	22.02	29.02
An	22.32	20.25	24.11	20.55	21.10	20.52
Lc	—	—	—	—	—	—
Ne	4.79	10.46	5.68	6.73	5.99	—
Di	16.31	20.29	18.69	16.05	15.75	12.26
Hy	—	—	—	—	—	2.62
Ol	18.00	18.10	18.63	19.76	18.31	15.35
Mt	2.64	2.77	3.22	4.13	4.25	3.67
Il	5.93	5.91	7.14	4.41	4.77	4.54
Ap	1.91	2.12	2.12	1.16	1.51	1.34
sample no. (P) ...	131	128	127	113	111	93
SiO_2	49.35	48.08	49.73	47.65	47.25	47.98
TiO_2	2.41	2.47	2.34	2.35	2.24	2.45
Al_2O_3	15.03	15.57	15.77	16.51	16.77	17.20
$Fe_2O_{3,\,tot}$	11.02	11.25	10.62	12.58	13.24	11.50
MnO	0.12	0.15	0.14	0.18	0.18	0.15
MgO	6.13	8.44	7.37	6.79	6.69	4.51
CaO	7.75	8.25	8.62	9.64	9.44	8.42
Na_2O	4.07	4.45	4.22	4.00	3.89	3.94
K_2O	1.98	1.83	1.68	0.99	0.99	1.18
P_2O_5	0.57	0.58	0.53	0.47	0.55	0.78
total	98.43	101.07	101.02	101.16	100.24	98.11
			trace elements			
Cr	211	257	247	166	173	83
Co	35	34	31	36	40	33
Ni	118	130	91	40	48	37
Cu	41	76	70	74	61	48
Zn	129	99	101	98	88	101
Pb	5	< 3	3	< 3	3	< 3
Rb	32	33	33	12	13	19
Sr	616	699	634	503	526	654
Y	21	20	20	24	25	32
Zr	172	196	168	167	166	188
Nb	43	42	34	21	20	31
Ba	400	422	379	260	260	482
			C.I.P.W. norms			
Qz	—	—	—	—	—	—
Or	12.00	10.82	9.93	5.85	5.91	7.15
Ab	32.18	22.57	28.36	25.36	29.40	34.35
An	17.31	17.07	19.09	24.14	25.60	26.53
Lc	—	—	—	—	—	—
Ne	1.68	8.12	3.93	4.55	4.43	—
Di	14.84	16.07	16.22	16.70	14.78	9.31
Hy	—	—	—	—	—	0.07
Ol	12.19	15.57	13.27	13.67	16.05	13.37
Mt	3.77	3.74	3.54	4.19	2.68	2.58
Il	4.69	4.69	4.44	4.46	4.29	4.79
Ap	1.37	1.37	1.25	1.11	1.30	1.89

PHILOSOPHICAL TRANSACTIONS OF THE ROYAL SOCIETY A MATHEMATICAL, PHYSICAL & ENGINEERING SCIENCES

TABLE 7 (*cont.*)

POST-PLATEAU (4–0.2 Ma).

sample no. (P) . . .	110	64	126	79	73	129
SiO_2	46.79	47.79	47.84	46.02	47.45	52.07
TiO_2	2.53	1.76	1.87	2.81	2.39	1.69
Al_2O_3	16.38	17.27	15.07	15.38	16.23	16.76
$Fe_2O_{3,\,tot}$	11.78	9.79	9.45	12.32	10.87	9.77
MnO	0.16	0.15	0.15	0.22	0.15	0.19
MgO	7.70	7.80	9.91	7.57	7.87	4.47
CaO	9.61	9.41	8.47	7.99	8.49	7.47
Na_2O	3.94	4.16	2.98	5.35	4.13	3.81
K_2O	1.18	1.04	3.85	1.72	1.86	1.53
P_2O_5	0.45	0.65	1.07	1.07	0.73	0.94
total	100.52	99.82	100.66	100.45	100.17	98.70
			trace elements			
Cr	261	173	359	243	274	252
Co	37	30	37	34	38	40
Ni	63	77	161	139	115	121
Cu	66	40	84	39	40	58
Zn	88	76	75	105	84	95
Pb	< 3	13	< 3	6	6	5
Rb	15	21	164	11	30	31
Sr	589	1082	752	1100	845	597
Y	20	20	18	30	21	20
Zr	154	155	450	435	223	191
Nb	26	20	25	109	40	3
Ba	233	300	385	609	424	393
			C.I.P.W. norms			
Qz	—	—	—	—	—	0.96
Or	6.97	6.21	22.76	10.23	11.05	9.22
Ab	21.56	24.67	11.21	19.37	21.69	32.91
An	23.60	25.67	16.40	12.94	20.42	24.68
Lc	—	—	—	—	—	—
Ne	6.47	5.88	7.59	14.21	7.32	—
Di	17.24	13.94	14.93	16.20	13.91	5.69
Hy	—	—	—	—	—	18.84
Ol	14.34	16.58	17.92	16.50	16.92	—
Mt	3.94	2.15	3.16	2.70	2.38	2.17
Il	4.82	3.38	3.55	5.37	4.58	3.29
Ap	1.06	1.56	2.52	2.55	1.75	2.26

sample no. (P) . . .	140	130	133	104	105	106
SiO_2	46.05	46.56	47.14	47.77	47.11	48.04
TiO_2	2.86	2.44	2.81	2.35	2.21	2.24
Al_2O_3	14.39	15.01	15.26	16.87	16.73	17.02
$Fe_2O_{3,\,tot}$	11.69	11.51	11.77	10.03	10.50	10.37
MnO	0.15	0.16	0.16	0.15	0.15	0.15
MgO	9.51	9.48	8.33	6.42	8.38	7.52
CaO	8.38	9.05	8.86	8.28	8.38	7.39
Na_2O	3.86	3.61	4.38	4.63	4.44	4.78
K_2O	2.09	2.28	1.98	2.11	2.03	2.02
P_2O_5	0.74	0.71	0.70	0.74	0.72	0.81
total	99.72	100.81	101.39	99.35	100.65	100.34

TABLE 7 (*cont.*)

sample no. (P) ...	140	130	133	104	105	106
			trace elements			
Cr	287	319	316	180	243	172
Co	42	43	40	32	37	31
Ni	167	165	115	68	101	100
Cu	61	74	75	57	60	51
Zn	117	109	113	85	79	78
Pb	6	<3	3	<3	7	5
Rb	32	55	31	39	38	33
Sr	796	746	834	811	818	825
Y	22	22	19	28	24	24
Zr	272	221	232	253	264	249
Nb	53	39	57	49	55	39
Ba	501	522	455	502	467	424
			C.I.P.W. norms			
Qz	—	—	—	—	—	—
Or	12.35	13.48	11.64	12.65	12.00	12.00
Ab	16.67	14.84	18.34	22.22	18.80	24.05
An	15.77	18.05	16.06	19.33	19.77	19.11
Lc	—	—	—	—	—	—
Ne	8.66	8.50	10.05	9.50	10.21	9.02
Di	16.89	17.88	18.62	14.22	13.79	10.11
Hy	—	—	—	—	—	—
Ol	8.29	17.21	14.46	13.59	16.06	17.29
Mt	2.97	3.84	3.90	2.22	3.51	2.26
Il	5.43	4.63	5.32	4.54	4.20	4.27
Ap	1.75	1.68	1.65	1.77	1.70	1.91

sample no. (P) ...	107	108	109	115	86	95
SiO_2	45.34	46.16	47.16	45.12	48.00	45.32
TiO_2	2.56	2.50	2.29	2.67	2.07	2.56
Al_2O_3	16.02	17.51	17.09	15.38	15.10	15.43
$Fe_2O_{3,\,tot}$	11.44	10.41	10.20	11.33	11.96	10.53
MnO	0.18	0.16	0.15	0.16	0.16	0.16
MgO	9.16	6.12	7.08	8.86	9.15	9.14
CaO	9.32	9.44	8.51	9.49	7.56	7.89
Na_2O	4.95	4.56	4.52	4.03	4.69	5.10
K_2O	1.86	2.01	2.13	2.30	1.12	2.81
P_2O_5	0.77	0.83	0.74	0.82	0.41	1.27
total	101.60	99.70	99.87	100.16	100.22	100.21
			trace elements			
Cr	258	119	185	303	275	249
Co	40	28	29	39	43	34
Ni	127	37	72	110	131	139
Cu	66	46	53	67	69	50
Zn	85	73	78	100	98	94
Pb	<3	8	10	<3	<3	4
Rb	39	41	40	44	20	49
Sr	816	893	841	899	376	1212
Y	21	27	24	21	22	28
Zr	245	262	271	257	128	396
Nb	65	58	55	70	20	92
Ba	537	550	480	689	289	689

PHILOSOPHICAL TRANSACTIONS OF THE ROYAL SOCIETY A MATHEMATICAL, PHYSICAL & ENGINEERING SCIENCES

TABLE 7 (*cont.*)

sample no. (P) . . .	107	108	109	115	86	95
			C.I.P.W. norms			
Qz	—	—	—	—	—	—
Or	10.93	12.00	12.71	13.71	6.62	16.73
Ab	10.35	15.90	19.78	10.26	26.27	9.92
An	15.91	21.67	20.26	17.20	17.00	10.98
Lc	—	—	—	—	—	
Ne	16.90	12.52	10.19	13.05	7.45	18.18
Di	20.10	16.48	14.08	19.93	14.71	16.16
Hy	—	—	—	—	—	
Ol	15.43	12.38	13.45	15.02	20.42	17.86
Mt	3.78	2.29	3.44	3.80	2.62	2.31
Il	4.82	4.80	4.39	5.11	3.95	4.90
Ap	1.79	1.98	1.77	1.96	0.97	3.02

sample no. (P) . . .	89	88	90
SiO_2	43.88	42.64	42.89
TiO_2	2.84	2.93	2.86
Al_2O_3	15.17	13.81	14.07
$Fe_2O_{3,\ tot}$	11.42	11.70	11.60
MnO	0.17	0.18	0.18
MgO	9.17	10.68	10.94
CaO	9.90	10.43	10.32
Na_2O	4.13	3.81	3.80
K_2O	2.28	2.38	2.27
P_2O_5	0.95	1.13	1.13
total	99.91	99.69	100.06
		trace elements	
Cr	291	435	397
Co	40	43	41
Ni	129	169	162
Cu	97	79	83
Zn	102	106	96
Pb	< 3	7	< 3
Rb	37	39	41
Sr	1054	1077	1155
Y	22	26	29
Zr	275	317	314
Nb	77	84	75
Ba	700	800	748
		C.I.P.W. norms	
Qz	—	—	—
Or	13.59	14.01	13.35
Ab	6.29	—	0.30
An	16.30	13.73	14.45
Lc	—	0.18	—
Ne	15.71	17.69	20.10
Di	21.70	25.15	23.76
Hy	—	—	—
Ol	14.90	18.36	20.13
Mt	3.84	2.58	1.80
Il	5.45	5.64	3.92
Ap	2.26	2.69	2.18

PHILOSOPHICAL TRANSACTIONS OF THE ROYAL SOCIETY A MATHEMATICAL, PHYSICAL & ENGINEERING SCIENCES

† *Notes on table 7*

Details of analysed specimens

124, 121, 129, 119, 117 (78–81 Ma), Quartz tholeiites, El Triunfo, 14 km W of Alto Rio Senguerr.
20, 18, 17 (77 Ma), Olivine tholeiites, Morro Negro, 8 km ESE of Coyhaique Alto.
71 (54 Ma), Olivine tholeiite, Cerro Lapiz, Chile Chico.
70 (57 Ma), Alkali basalt, Cerro Lapiz, Chile Chico.
69, 68 (52 Ma), Olivine tholeiites, Cerro Lapiz, Chile Chico.
40 (46 Ma), Alkali basalt, 3 km SSW of Balmaceda airport.
67, (43 Ma), Basanite, Cerro Lapiz section, Chile Chico.
66 (43 Ma), Alkali basalt, immediately beneath tuffaceous horizon P65.
144, Alkali basalt, Sierra Corrientes, 6 km ENE of Ea Molle Grande.
136, Alkali basalt, Cerro San Bernardo.
132 (21 Ma), Olivine tholeiite, 15 km SE of Facundo.
131 (22 Ma), Alkali basalt, 15 km SE of Facundo.
128, Alkali basalt, 15 km S of Los Tamariscos.
127 (20 Ma), Alkali basalt, 13 km SE of Los Tamariscos.
113, Alkali basalt, Ea La Vizcaina, south side of Meseta del Lago Buenos Aires.
111 (10 Ma), Alkali basalt, extensive flow at top of plateau Ea La Vizcaina.
93 (10 Ma), Olivine tholeiite, top of Meseta Gambarana.
110 (9 Ma), Alkali basalt, edge of plateau above Ea Vizcaina, southeast side of Meseta del Lago Buenos Aires.
64, Alkali basalt, flow on surface of plateau, Cerro Lapiz, Chile Chico.
126, Alkali basalt, 2 km E of Ea Arroyo Gato.
79, Basanite, lava forming Cerro Lapiz, Chile Chico.
73, Alkali basalt, flow from Pico Sur, Chile Chico.
129 (3.2 Ma), Quartz tholeiite, 24 km S of Los Tamariscos.
140, Alkali basalt, edge of plateau N of Brazo Norte.
130 (2.6 Ma), Alkali basalt, 2 km N of Salina Grande, Ea. Alberdi.
133 (2.7 Ma), Basanite, Cerro del Pulgas, Facundo-Sarmiento Road.
104, Alkali basalt, 1 km S of Puesto El Perdido, Meseta del Lago Buenos Aires.
105, Basanite, 8 km S of Puesto El Perdido, Meseta del Lago Buenos Aires.
106, Alkali basalt, lowest flow in crater wall Laguna Honda, Meseta del Lago Buenos Aires.
107, Basanite, 20 m above 106, Meseta del Lago Buenos Aires.
108, Basanite, 10 m above 107, Meseta del Lago Buenos Aires.
109, Basanite, top flow in crater wall of Laguna Honda, Meseta del Lago Buenos Aires.
115 (0.8 Ma), Basanite, track to Ea Vizcaina, SE of Meseta del Lago Buenos Aires.
86, Alkali basalt, 2 km SE of Perito Moreno.
95, Basanite, Ruta 40, 6 km S of Rio Telken.
89, Basanite, Ea Laurak Bat.
88 (0.3 Ma), Leucite basanite, flow from Cerro Volcan, 11 km SE of Perito Moreno.
90 (0.2 Ma), Leucite basanite, Arroyo Page, 17 km ESE of Perito Moreno.

Chico lavas. One other difference between the two oldest sections is that K_2O is appreciably higher in the more northerly Senguerr group than in the contemporaneous lavas of Morro Negro. Lavas of both sections have tholeiitic characteristics with some calc-alkaline affinity but Senguerr lies only slightly east of Morro Negro, which lends little credibility to any suggestion that this is a reflection of a K_2O–depth relation above an easterly dipping subduction zone.

The normative Di–Ol–Ne–Hy–Qz plot (figure 16) illustrates the compositional spread of the Patagonian lavas in terms of major normative constituents and shows that, with occasional exceptions, the early basalts are of tholeiitic composition and the later ones undersaturated, tending to become more nepheline-normative with time.

Relatively few systematic variations were evident in plots of trace elements against major components such as SiO_2 or MgO. Plots with Ti, Zr, Y and Sr, as devised by Pearce & Cann (1973), were used particularly in an attempt to determine the affinities of the earliest lavas: the strongly alkalic nature of the middle and upper parts of the sequence is more readily apparent. These plots reinforce the suggestion that lavas from the Senguerr and Morro Negro sections,

which both date at approximately 80 Ma, tend to have characteristics that separate them from the rest of the plateau. With Y/Nb ratios (Pearce & Cann 1973) these lavas would be classified as tholeiitic whereas almost all of the remainder are alkalic: the exception is one early plateau lava from Chile Chico (P69) which has a Y/Nb ratio of 1.7, and on this basis would be regarded as transitional in character. Ratios of Y/Nb are plotted against Sr in figure 17.

In the Ti–Zr–Y triangle it is again apparent that the Morro Negro and Senguerr lavas plot in clusters separate from the other lavas (figure 18). They fall within or very close to the area occupied dominantly by calc-alkali basalts: most of the remaining lavas fall within the field of 'within-plate' basalts. The Morro Negro and Senguerr basalts are also plotted in the Ti–Zr–Sr

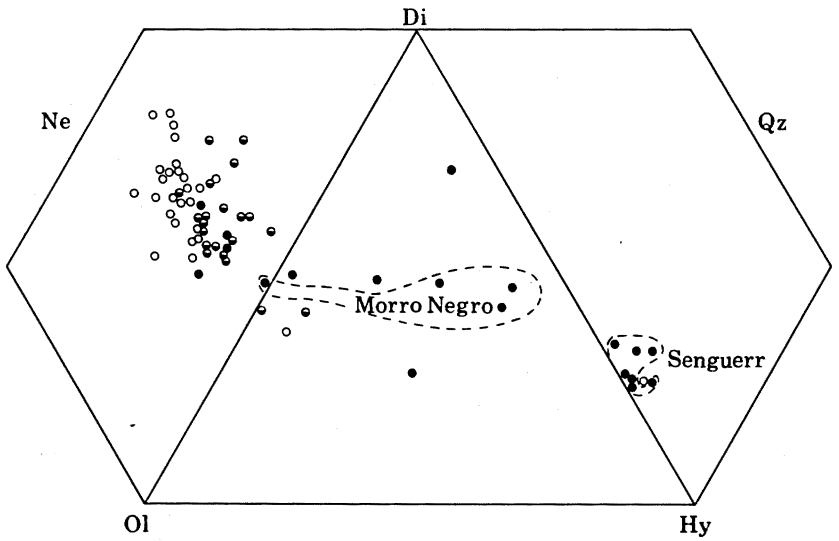

FIGURE 16. Plot of normative diopside–olivine–nepheline–hypersthene–quartz illustrating compositional spread of the Patagonian lavas. Quartz tholeiites and olivine tholeiites predominate in the older sections of Senguerr and Morro Negro respectively. ●, Early plateau; ◒, late plateau; ○, post-plateau.

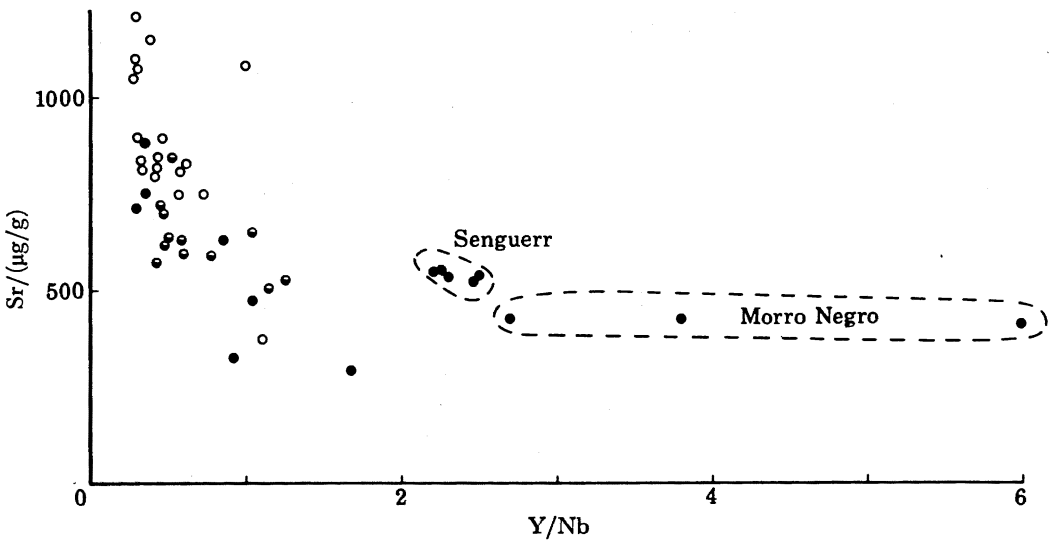

FIGURE 17. Plot of Y/Nb against Sr in which the older lavas of Senguerr and Morro Negro are distinguished from the remainder of the plateau basalts. Symbols are as in figure 16.

triangle (figure 19) which though less reliable because of the possibility of Sr mobility nevertheless points to calc-alkali affinity.

The Ti–Zr plot (Pearce & Cann 1973) is not strictly applicable in this instance since the Patagonian lavas are relatively enriched in both elements and fall largely outside the limits that were originally used on this diagram. For this reason, the field boundaries of Pearce & Cann have been omitted, but the plot illustrates (figure 20) that once again the Senguerr and Morro Negro groups are distinct from the rest and show calc-alkali tendencies. They are displaced towards lower Ti values and for Senguerr to higher Zr as well.

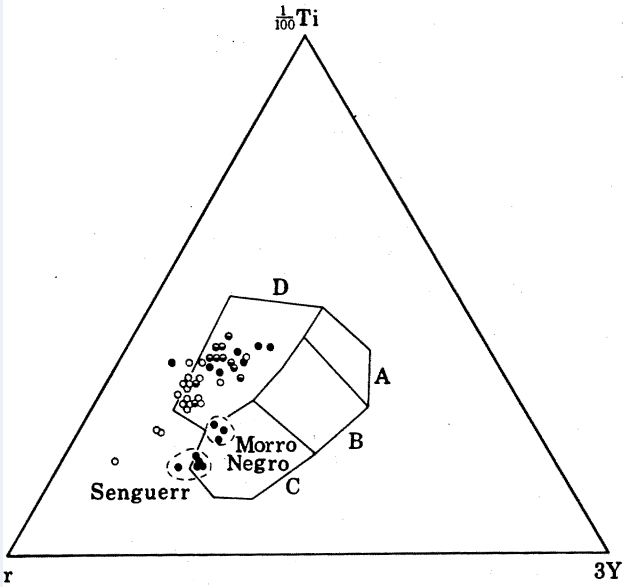

FIGURE 18. Ti–Zr–Y discrimination diagram (after Pearce & Cann 1973). The older tholeiitic basalts of Senguerr and Morro Negro plot in or close to field C (calc-alkali basalts). Most of the remaining Patagonian lavas plot in field D (within-plate basalts). Low-K tholeiites tend to plot in field A, and ocean-floor basalts in field B. Symbols are as in figure 16.

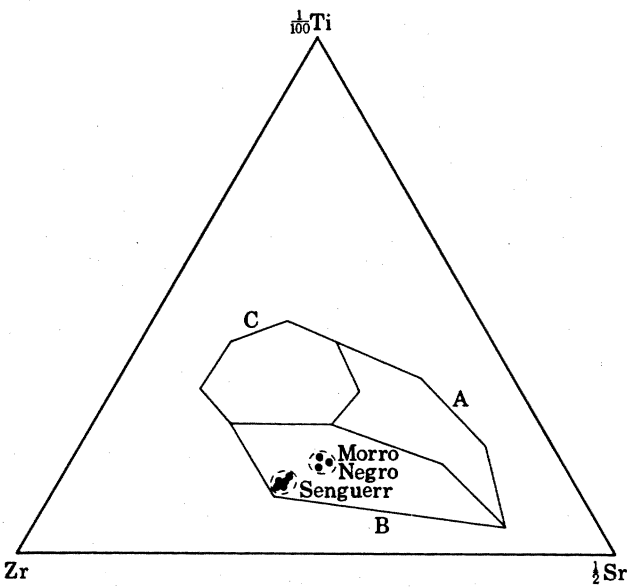

FIGURE 19. Ti–Zr–Sr discrimination diagram (after Pearce & Cann 1973) illustrating how the older lavas of Senguerr and Morro Negro fall within field B (calc-alkali basalts). Low K tholeiites tend to plot in field A and ocean floor basalts in field C. Symbols are as in figure 16.

There is some systematic covariance of certain minor or trace-element pairs in the alkali basalts and basanites. For example, there is a strong positive correlation between Nb and P and a less marked one between Nb and Rb. Plots of both Rb and K against Zr (figure 21) also show positive correlation but tend to separate more westerly lavas with relatively low K and Rb for a given Zr content from those to the east which have higher concentrations of these elements. Incompatible elements are generally enriched in the late and post-plateau basanites relative to the less undersaturated earlier lavas.

Mantle-normalized trace-element distribution patterns were used by Hawkesworth *et al.* (1979) to contrast the Patagonian lavas with the calc-alkaline andesites of Ecuador and northern Chile. The alkali basalts and basanites conform to a fairly constant pattern of trace-element variations showing varying degrees of enrichment relative to 'mantle' values (figure 22). A basanite low in the succession (P67) shows a similar pattern to late basanites except for slight

depletion in K and Rb. The flow most enriched in incompatible elements is the late basanite P95, from Rio Telken.

Early Patagonian tholeiites are generally more enriched in incompatible and other trace elements when compared with ocean floor basalts (Kay & Hubbard 1978) and with the marginal basin basalts of Sarmiento (Tarney *et al.* 1976). The patterns for the Patagonian tholeiites (figure 23) are unlike those for the overlying alkalic rocks and resemble those for the marginal-basin basalts showing relative depletion in Nb, Rb and Sr and enhancement of Zr and Y. The

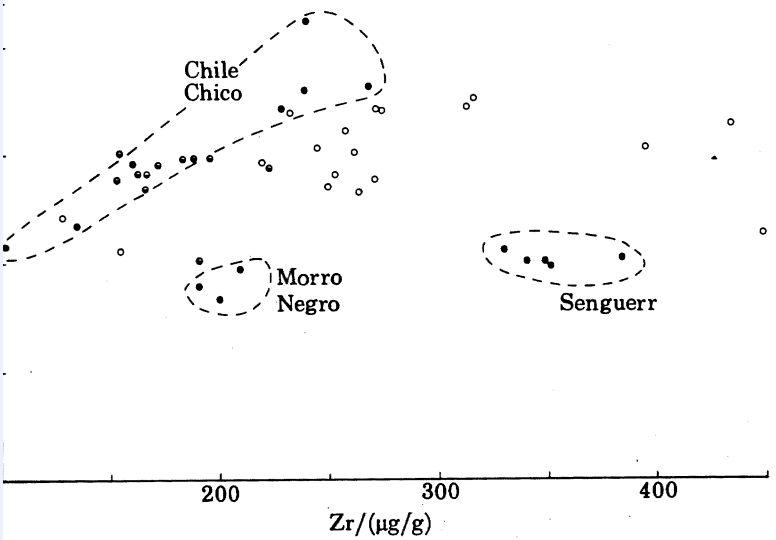

FIGURE 20. Plot of Ti against Zr for the Patagonian plateau basalts. Note the generally lower Ti-values on the older lavas of Senguerr and Morro Negro, which is again a calc-alkali characteristic (cf. Pearce & Cann 1973, figure 2, p. 295). Symbols are as in figure 16.

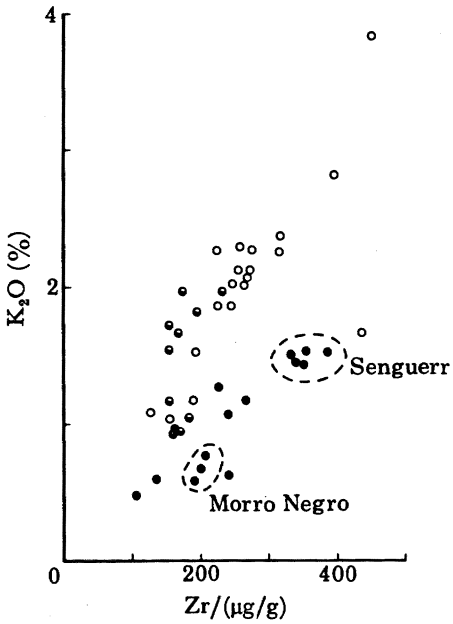

FIGURE 21. Plot of K_2O against Zr for Patagonian basalts. Symbols are as in figure 16.

trace-element patterns for the Patagonian tholeiites differ from those found in calc-alkali rocks such as the Jurassic volcanics of the adjacent cordillera (table 2, no. 1) or those for the Lesser Antilles island-arc (for example, St Kitts and Dominica basalts (Brown *et al.* 1977, p. 790). The trace-element pattern for one of the young tholeiites (P129 from near Los Tamariscos) bears a closer resemblance to those of the post-plateau alkali basalts than it does to the earlier tholeiites.

Strontium isotope ratios for the Patagonian lavas were reported by Hawkesworth *et al.* (1979) who found the observed range for $^{87}Sr/^{86}Sr$ to be 0.7034–0.7052. Six new determinations coincide with the previously established range (table 8). The isotopic ratios did not appear to vary systematically with geographical or stratigraphical position, with petrography or trace-element chemistry.

On the $^{143}Nd/^{144}Nd$ against $^{87}Sr/^{86}Sr$ plot (Hawkesworth *et al.* 1979, p. 52, figure 5) two of these three lavas fall within the field of Icelandic basalts, approaching the position occupied by the back-arc basalts of the Scotia Sea which are only slightly removed from m.o.r.b. ratios.

Chondrite-normalized r.e.e. distribution patterns (Hawkesworth *et al.* 1979, p. 49, figure 3)

show consistent light r.e.e. enrichment, which is more conspicuous in the basanites than in the alkali basalts or tholeiite. The correlation between $^{87}Sr/^{86}Sr$ and Rb/Sr and between $^{143}Nd/^{144}Nd$ and Sm/Nd for three samples from the Perito Moreno area suggested an 'age' of 500 Ma which was taken to indicate that heterogeneities had persisted in the source over that period of time. The trace-element and isotopic geochemistry was thought to be a function of the source rocks rather than the melting processes. The apparent coherence of Rb/Sr with Sm/Nd was taken as evidence that the lavas represented 'reasonable degrees of partial melting' (i.e. more than 5 %).

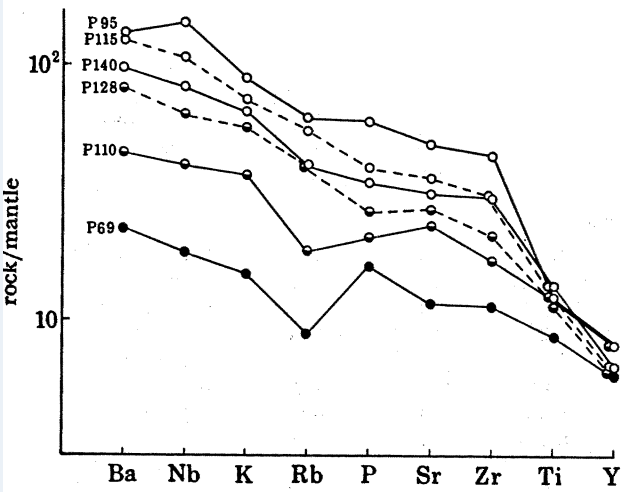

FIGURE 22. Mantle-normalized trace-element distribution patterns for an olivine tholeiite (P69), alkali basalts (P110, P128) and basanites (P140, P115 and P95) from the Patagonian plateau. 'Mantle' values derived from Hawkesworth *et al.* (1979) and Kay & Hubbard (1978). Symbols are as in figure 16.

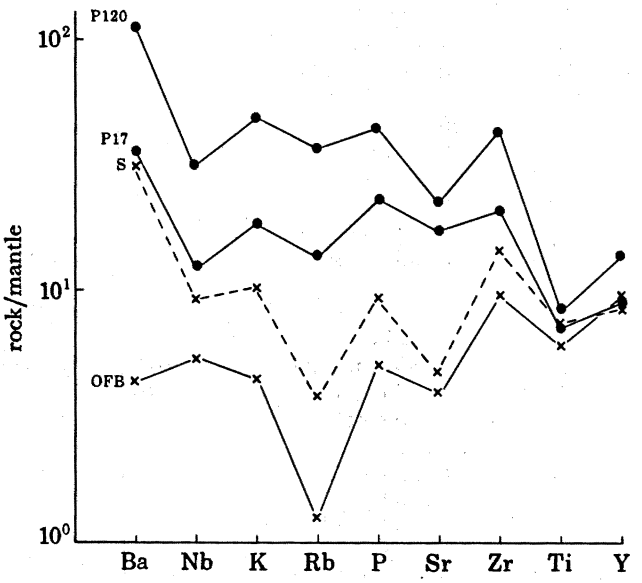

FIGURE 23. Mantle-normalized trace-element distribution patterns for older lavas of the Patagonian plateau. P17 is an olivine tholeiite from Morro Negro, and P120 a quartz tholeiite from Senguerr. S is a pillow lava from the Sarmiento marginal basin (Tarney *et al.* 1978) and OFB an ocean floor basalt (Kay & Hubbard 1978). 'Mantle' values were derived as in figure 22.

Hawkesworth *et al.* also demonstrated that the coherent variation of Nd and Sr isotopes in the Patagonian volcanics is similar to that observed in Atlantic volcanic rocks while calc-alkali rocks are displaced to more radiogenic compositions. The relative enrichment of calc-alkali lavas in alkaline elements (K, Rb and Sr) relative to the rare earths was attributed to the influence of H_2O-rich fluids derived from subducted lithosphere.

DISCUSSION

The basalts of the Aisen, Chubut and Santa Cruz provinces described in this paper show a span of ages from 80 Ma to near-historic and embrace the maximum age-range so far reported for the entire Patagonian plateau (Ramos *et al.* 1980). They may be divided into four groups which have both age and compositional significance:

(i) The earliest (*ca.* 80 Ma) basalts are tholeiitic in terms of their major-element chemistry and also on the basis of Y/Nb ratios, but on Ti–Zr–Y and Ti–Zr plots they appear to have

calc-alkaline affinities. However, on the basis of mantle-normalized trace element patterns they appear less like calc-alkali rocks and show more resemblance to marginal-basin basalts such as those of the Sarmiento complex (Tarney *et al.* 1976).

(ii) The basalts of the Chile Chico section (43–56 Ma) range from olivine tholeiites to basanites in their major-element compositions, and in their mantle-normalized trace-element patterns show a range of characteristics intermediate between ocean-floor and marginal-basin basalts

TABLE 8. STRONTIUM ISOTOPE RATIOS IN PATAGONIAN LAVAS

sample no.	petrographic type	age Ma	SiO_2 (%)	K_2O (%)	Rb µg/g	Sr µg/g	$^{87}Sr/^{86}Sr$
P90	leucite basanite	0.2	42.9	2.61	41	1155	0.70443 ± 4
P88	leucite basanite	0.3	42.6	2.38	39	1077	0.70445 ± 3
P40	alkali basalt	—	45.1	1.19	22	713	0.70338 ± 5
P95	basanite	—	45.3	2.81	49	1212	0.70451 ± 2
P89	basanite	—	43.9	2.28	37	1054	0.70447 ± 4
P108	basanite	—	46.2	2.01	41	893	0.70465 ± 3
P140	basanite	3.0	46.1	2.09	32	796	0.70525 ± 4
P129	quartz tholeiite	3.2	52.1	1.53	31	597	0.70526 ± 5
P126	alkali basalt	—	47.9	3.85	64	752	0.70477 ± 6
			plateau surface				
P110	basanite	9.0	46.8	1.18	15	589	0.70403 ± 4
P93	olivine tholeiite	10	48.0	1.18	19	654	0.70379 ± 6
P111	alkali basalt	10	47.3	0.99	13	526	0.70419 ± 2
P113	alkali basalt	—	47.7	0.99	12	503	0.70421 ± 3
P143	basanite	25	45.5	1.47			0.70399 + 12
P136	alkali basalt	—	45.5	1.05	19	715	0.70393 ± 5
P144	alkali basalt	—	45.5	1.55	23	631	0.70418 + 6
P69	olivine basalt	—	45.3	0.48	7	294	0.70353 ± 3
P71	olivine tholeiite	55	47.5	1.29	18	626	0.70394 ± 3
P124	quartz tholeiite	78	51.8	1.51	29	536	0.70443 ± 3
P117	quartz tholeiite	82	51.7	1.44	27	540	0.70443 ± 4
P20	olivine tholeiite	—	50.9	0.67	16	414	0.70381 ± 5

on the one hand, and the more enriched patterns exhibited by the younger alkali basalts and basanites on the other. The most depleted trace-element distribution is found in a quartz tholeiite from this section (P69) which bears a similarity to the pattern for an ocean-floor basalt (figure 23).

(iii) The upper part of the plateau (9–25 Ma) is composed chiefly of alkali basalts, with occasional basanites and tholeiites. They have broadly similar fairly enriched mantle-normalized incompatible trace-element and rare-earth-element patterns.

(iv) The post-plateau lavas (0.2–4 Ma) are generally more undersaturated and include leucite-bearing basanites. They are low-silica lavas enriched with incompatible trace elements. These lavas are more alkalic and more extreme in composition than the Pleistocene to Recent lavas of Palei-Aike from the southern part of Patagonia described by Skewes & Stern (1979).

One interpretation is that the earlier tholeiitic lavas of Morro Negro and Senguerr may be more closely related to a subduction regime since they show some calc-alkali characteristics (see, for example, figures 18 and 19) and also have some features of marginal basin basalts (for example trace-element patterns in figure 23). The initial stages of volcanism may therefore have corresponded to a back-arc situation which seems to have reached its maximum during the eruption of the early Chile Chico lavas, especially the olivine tholeiite (P69) which has a low

$^{87}Sr/^{86}Sr$ ratio (0.70353 ± 3) and shows the greatest depletion in r.e.e. and l.i.l. elements. The limited Sr and Nd isotope data available (there are no Nd figures for the Senguerr and Morro Negro lavas) do not show the displacement to more radiogenic values which is seemingly characteristic of calc-alkali suites (Hawkesworth *et al.* 1979, p. 52). Back-arc basalts would in any case, seem to fall on the same trend exhibited by oceanic and continental volcanics. In contrast with the earlier eruptives there is no suggestion of any marginal basin or calc-alkali influence when volcanic activity resumed at approximately 25 Ma.

With rare exceptions the late and post-plateau lavas are decidedly alkaline and of continental intra-plate type. It has been suggested (Baker & Rea 1978) that the Patagonian volcanism may have developed in an extensional régime created as an indirect response to subduction and that it may represent incipient crustal rifting in a type of back-arc environment. Similarly Skewes & Stern (1979) have suggested that the volcanism may be '. . . related to thermal or mechanical perturbation of the subcontinental mantle due to subduction'. Apart from their geographic and tectonic situation, east of the cordillera, there is little to connect the later Patagonian volcanics with orogenic processes. The precise nature of any link with subduction, if it exists, must for the time being remain a matter for speculation.

The expedition was planned under the auspices of the Cold Temperate South-American Subcommittee (Chairman, Sir Vivian Fuchs, F.R.S.) of the Southern Zone Research Committee of the Royal Society. We acknowledge with thanks the financial and administrative support of the Royal Society, CONICET (Argentina) and CONICYT (Chile). In particular we thank Mr G. Hemmen, Dr R. W. J. Keay, Sir Kingsley Dunham, F.R.S., Mr N. A. W. Le Grand, Sr̃ V. H. Cicardo, Sr̃ Ciarrapico and Sr̃ F. Rudloff. For logistic support we thank the Servicio Geologico Nacional of Agentina and the Instituto de Investigaciones Geologicas of Chile. We are grateful for the help we received from the British Council which played a vital liaison role in organizing the expedition: our thanks especially to Dr D. J. Boak in Buenos Aires and Dr V. Atkinson in Santiago. We are indebted to Professor O. Gonzalez-Ferran, formerly Director of the Instituto de Investigaciones Geologicas, for looking after much of the organization in Chile and for his most valuable contribution to the field work. We also thank our other colleagues in the field: Dr V. Covacevich, Dr E. Gonzalez-Diaz, Sr̃ R. Bustos, Sr̃ O. Perez and Sr̃ Blik. For their help and hospitality we thank Sr̃ Leandro de los Hoyos, Sr̃ Mirabelli, and other members of the Plan Patagonia Comahue in Comodoro Rivadavia. We also record our appreciation of the kindness and generosity shown to us at many Patagonian estancias during the course of the expedition. Finally, we thank Mr A. R. Gledhill for his help with the isotopic work and Mr A. Gray for the X-ray fluorescence analyses at Leeds University.

References

Abbey, S. 1978 Calibration Standards. IV. Studies in standard samples: for use in the general analysis of silicate rocks and minerals, part 5. 1977 edn of 'Usable' values. *X-Ray Spectrom.* **7**, 99–121.

Baker, P. E. & Rea, W. J. 1978 Compositional variations in the Patagonian plateau basalts. Abstract in *International Geodynamics Conference, Tokyo*, pp. 206–207. Tokyo: Science Council of Japan.

Brown, G. C. 1977 Mantle origin of Cordilleran granites. *Nature, Lond.* **265**, 21–24.

Brown, G. M., Holland, J. G., Sigurdsson, H., Tomblin, J. F., & Arculus, R. J. 1977 Geochemistry of the Lesser Antilles volcanic island arc. *Geochim. cosmochim. Acta* **41**, 785–810.

Charrier, R., Linares, E., Niemeyer, H. & Skarmeta, J. 1978 Edades potasio–argon de vulcanitas Mesozoicas y Cenozoicas del sector Chileno de la Meseta Buenos Aires, Aysen, Chile y su significade geologico. *Proc. VII Congreso Geologico Argentino, Neuquén*, vol. II, pp. 23–41.

PHILOSOPHICAL TRANSACTIONS OF THE ROYAL SOCIETY A MATHEMATICAL, PHYSICAL & ENGINEERING SCIENCES

Charrier, R., Linares, E., Niemeyer, H. & Skarmeta, J. 1979 K–Ar ages of basalt flows of the Meseta Buenos Aires in southern Chile and their relation to the southeast Pacific triple junction. *Geology* **7**, 436–439.
Cox, K. G. 1972 The Karroo volcanic cycle. *J. geol. Soc. Lond.* **128**, 311–36.
Cummings, D. & Schiller, G. I. 1971 Isopach map of the Earth's crust. *Earth Sci. Rev.* **7**, 97–125.
Dalziel, I. W. D., de Wit, M. J. & Palmer, K. F. 1974 Fossil marginal basin in the Southern Andes. *Nature, Lond.* **250**, 291–294.
Dalziel, I. W. D., de Wit, M. J. & Ridley, W. I. 1975 Structural and petrological studies in the Scotia Arc and Patagonian Andes. *Antarct. J. U.S.* **10**, 307–310.
De Wit, M. 1977 The evolution of the Scotia Arc as a key to the reconstruction of Southwestern Gondwanaland. *Tectonophysics* **37**, 53–81.
Eichelberger, J. C. 1978 Andesitic volcanism and crustal evolution. *Nature, Lond.* **275**, 21–27.
Ewart, A., Taylor, S. R. & Capp, A. C. 1968 Trace and minor element geochemistry of the rhyolitic volcanic rocks, Central North Island, New Zealand. *Contr. Miner. Petr.* **18**, 76–104.
Farrar, E. H., Clark, S. J., Haynes G. S., Quirt, H., Conn, H. & Zentilli, M. 1970 K–Ar evidence for the post-Paleozoic migration of granitic intrusion foci in the Andes of northern Chile. *Earth planet. Sci. Lett.* **10**, 60–66.
Gass, I. G., Chapman, D. S., Pollack, H. N. & Thorpe, R. S. 1978 Geological and geophysical parameters of mid-plate volcanism. *Phil. Trans. R. Soc. Lond.* A **288**, 581–597.
Ghose, N. C. 1976 Composition and origin of Deccan basalts. *Lithos* **9**, 65–73.
Gonzales, B. F. & Aguirre, L. 1968 The metamorphic crystalline basement of Chile. Abstract in *23rd International Geological Congress, Czechoslovakia*, vol. 108. Prague: Academia.
Halpern, M. 1973 Regional geochronology of Chile south of 50° latitude. *Bull. geol. Soc. Am.* **84**, 2407–2422.
Halpern, M. & Fuenzalida, R. 1978 Rubidium–strontium geochronology of a transect of the Chilean Andes between latitudes 45° and 46 °S. *Earth planet. Sci. Lett.* **41**, 60–66.
Halpern, M., Stipanicic, P. N. & Toubes, R. O. 1975 Geochronologia (Rb/Sr) en los Andes Australes Argentinos. *Revta Asoc. geol. argent.* **30**, 180–192.
Harris, D. M. 1977 Ascent and crystallization of albite and granitic melts saturated with H_2O. *J. Geol.* **85**, 451–459.
Hawkesworth, C. J., Norry, M. J., Roddick, J. C., Baker, P. E., Francis, P. W. & Thorpe, R. S. 1979 $^{143}Nd/^{144}Nd$, $^{87}Sr/^{86}Sr$, and incompatible element variations in calc-alkaline andesites and plateau lavas from South America. *Earth planet. Sci. Lett.* **42**, 45–57.
Hawkesworth, C. J., O'Nions, R. K., Pankhurst, R. J., Hamilton, P. J. & Evensen, N. M. 1977 A geochemical study of island-arc and back-arc tholeiites from the Scotia Sea. *Earth planet. Sci. Lett.* **36**, 253–262.
Kay, R. W. & Hubbard, N. J. 1978 Trace elements in ocean ridge basalts. *Earth planet Sci. Lett.* **38**, 95–116.
Kramers, J. D. 1977 Lead and strontium isotopes in Cretaceous kimberlites and mantle-derived xenoliths from southern Africa. *Earth planet. Sci. Lett.* **34**, 419.
Kushiro, I. 1960 Si–Al relations in clinopyroxenes from igneous rocks. *Am. J. Sci.* 258, 548–554.
Kushiro, I. 1969 The system forsterite–diopside–silica with and without water at high pressures. *Am. J. Sci.* **267**A, 269–294.
Larson, R. L. & Pitman, W. C. III 1972 World-wide correlation of Mesozoic magnetic anomalies and its implications. *Bull. geol. Soc. Am.* **83**, 3645–3662.
Le Bas, M. J. 1962 The role of aluminium in igneous clinopyroxenes with relation to their parentage. *Am. J. Sci.* **260**, 267–288.
Le Maitre, R. W. & Gass, I. G. 1963 Occurrence of leucite in volcanic rocks from Tristan da Cunha. *Nature, Lond.* **198** (4882), 779–80.
Lopez-Escobar, L., Frey, F. A. & Vergara, M. 1977 Andesites and high-alumina basalts from the central-south Chile High Andes: geochemical evidence bearing on their petrogenesis. *Contr. Miner. Petr.* **63**, 199–228.
Ludwig, W. J., Ewing, J. I. & Ewing, M. 1968 Structure of the Argentine continental margin. *Bull. Am. Ass. Petrol. Geol.* **52**, 2337.
Molnar, P. & Atwater, T. 1978 Interarc spreading and cordilleran tectonics as alternates related to the age of subducted oceanic lithosphere. *Earth planet. Sci. Lett.* **41**, 330–340.
O'Hara, M. J. 1977 Geochemical evolution during fractional crystallization of a periodically refilled magma chamber. *Nature, Lond.* **266**, 503–507.
Oxburgh, E. R. & Parmentier, E. M. 1977 Compositional and density stratification in oceanic lithosphere – causes and consequences. *J. geol. Soc. Lond.* **133**, 343–356.
Pearce, J. A. 1975 Basalt geochemistry used to investigate past tectonic environment on Cyprus. *Tectonophysics* **25**, 41–68.
Pearce, J. A. & Cann, J. R. 1973 Tectonic setting of basic volcanic rocks determined using trace element analyses. *Earth planet. Sci. Lett.* **19**, 290–300.
Pearce, J. A. & Gale, G. H. 1977 Identification of ore-deposition environment from trace-element geochemistry of associated igneous host rock. In *Volcanic processses in ore genesis. Geol. Soc. Lond. Publ.* **7**, 14–24.
Pichler, H. & Zeil, W. 1972 The Cenozoic rhyolite–andesite associations of the Chilean Andes. *Bull. volcan.* **35**, 424–452.

PHILOSOPHICAL TRANSACTIONS OF THE ROYAL SOCIETY A MATHEMATICAL, PHYSICAL & ENGINEERING SCIENCES

PHILOSOPHICAL TRANSACTIONS OF THE ROYAL SOCIETY A MATHEMATICAL, PHYSICAL & ENGINEERING SCIENCES

PHILOSOPHICAL TRANSACTIONS OF THE ROYAL SOCIETY A MATHEMATICAL, PHYSICAL & ENGINEERING SCIENCES

IGURE 7. Small basalt meseta showing trap features overlying Mesozoic ignimbrite (cliffs in foreground); Cueva de los Manos 47° 10′S, 70° 28′W.

FIGURE 8. Patagonian basalts at Chile Chico, cut by the Cerro Lapiz plug, a locality for ultramafic xenoliths.

PHILOSOPHICAL TRANSACTIONS OF THE ROYAL SOCIETY A MATHEMATICAL, PHYSICAL & ENGINEERING SCIENCES

FIGURE 10. Cerro Colorado and other post-plateau cones on surface of Meseta del Lago Buenos Aires; basanite flow in foreground.

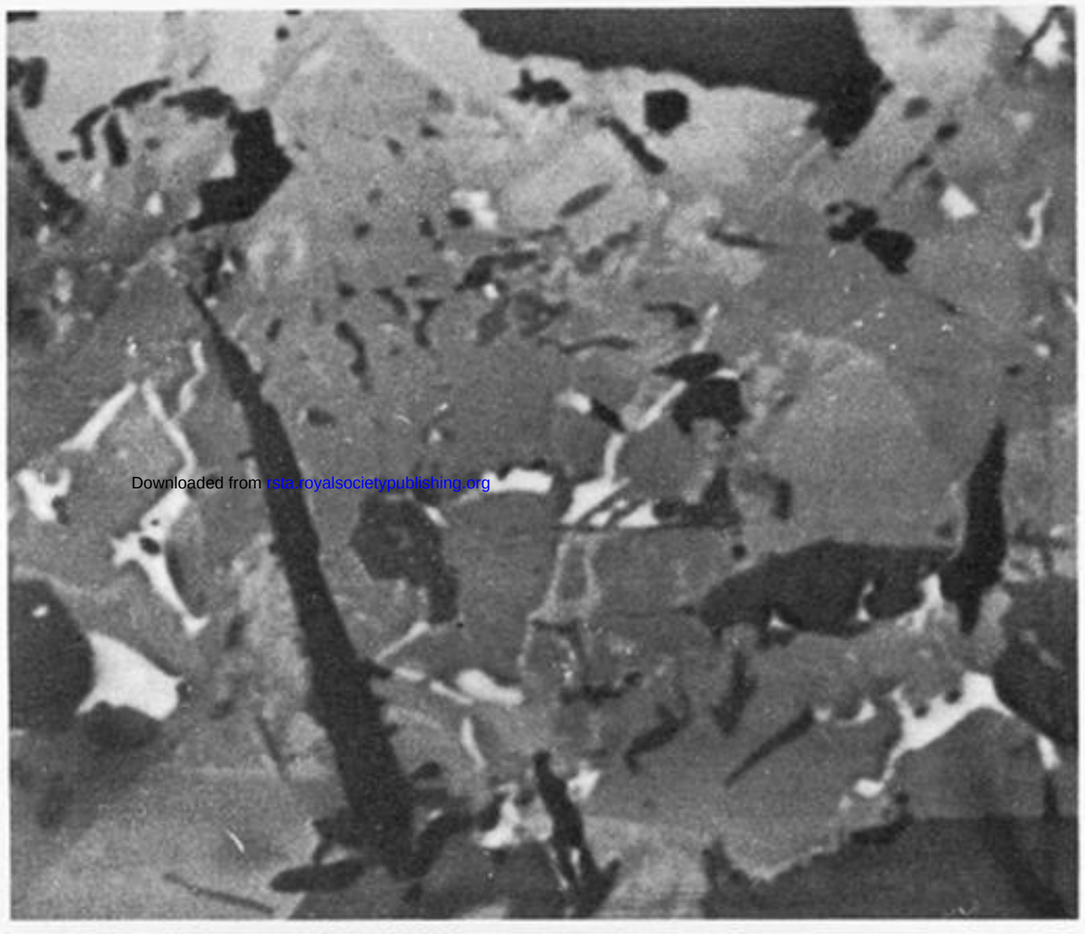

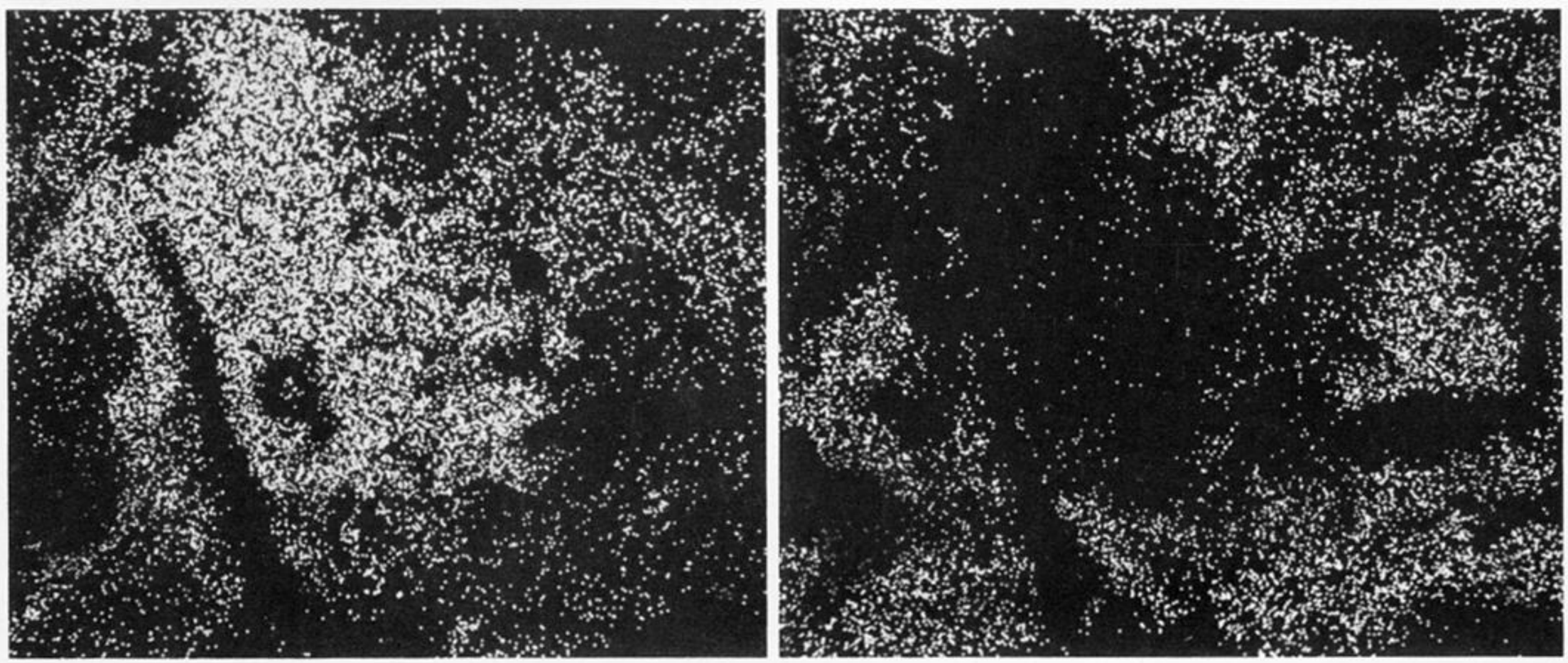

FIGURE 11. Electron microprobe images illustrating occurrence of leucite (high K and low Na concentrations) in basanite P90: top, back-scattered electron image; bottom left, K distribution; bottom right, Na distribution.

PHILOSOPHICAL TRANSACTIONS OF THE ROYAL SOCIETY A MATHEMATICAL, PHYSICAL & ENGINEERING SCIENCES